

pubs.acs.org/crystal Article

## Pharmaceutical Digital Design: From Chemical Structure through Crystal Polymorph to Conceptual Crystallization Process

Published as part of Crystal Growth & Design virtual special issue "Industrial Crystallization: ISIC 22/BACG 52".

Christopher L. Burcham,\* Michael F. Doherty, Baron G. Peters, Sarah L. Price, Matteo Salvalaglio, Susan M. Reutzel-Edens, Louise S. Price, Ravi Kumar Reddy Addula, Nicholas Francia, Vikram Khanna, and Yongsheng Zhao



Cite This: Cryst. Growth Des. 2024, 24, 5417-5438



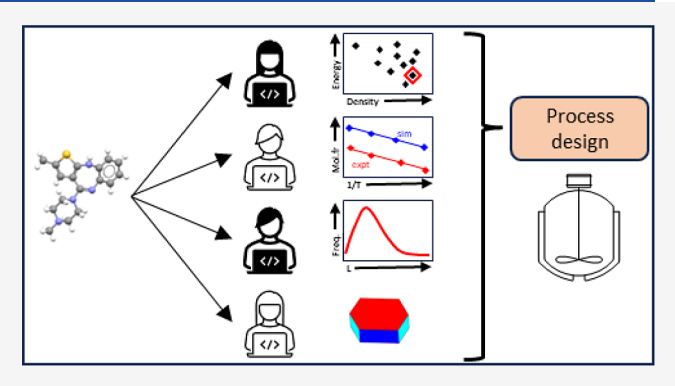
**ACCESS** I

III Metrics & More

Article Recommendations

Supporting Information

ABSTRACT: A workflow for the digital design of crystallization processes starting from the chemical structure of the active pharmaceutical ingredient (API) is a multistep, multidisciplinary process. A simple version would be to first predict the API crystal structure and, from it, the corresponding properties of solubility, morphology, and growth rates, assuming that the nucleation would be controlled by seeding, and then use these parameters to design the crystallization process. This is usually an oversimplification as most APIs are polymorphic, and the most stable crystal of the API alone may not have the required properties for development into a drug product. This perspective, from the experience of a Lilly Digital Design project, considers the fundamental theoretical basis of crystal structure prediction (CSP), free energy, solubility,



morphology, and growth rate prediction, and the current state of nucleation simulation. This is illustrated by applying the modeling techniques to real examples, olanzapine and succinic acid. We demonstrate the promise of using ab initio computer modeling for solid form selection and process design in pharmaceutical development. We also identify open problems in the application of current computational modeling and achieving the accuracy required for immediate implementation that currently limit the applicability of the approach.

## 1. INTRODUCTION

The development of a new pharmaceutical product begins with the hypothesis that a new molecule will either promote or interrupt a biochemical pathway to affect a disease state. The target molecule is tested in clinical trials for safety (Phase I) and both safety and efficacy (Phase II and III) and ultimately progresses to the commercialization of a new medicine if successful. The journey for a molecule to become a medicine is long, usually fraught with many obstacles, and very expensive. The average cost to develop a new drug has been estimated to be between \$2.3 billion (reported in 2023)<sup>1,2</sup> and \$3 billion (reported in 2013),3 with the probability that a Phase I compound will successfully progress to product approval at just under 12%.3

Computational tools are regularly used by pharmaceutical companies in the initial phase of drug discovery, e.g., to predict medicinal chemistry targets and pathways, 4-6 identify candidate molecules and compute binding affinity, 7,8 metabolism,9 and toxicological issues.10,11 These efforts help identify

promising candidates and guide subsequent experimental efforts.

Product and process development remains largely empirically and experimentally driven, though the utilization of mechanistic models has been increasing. Pharmacokinetic and pharmacodynamic (PK-PD) models are now widely used to predict in vivo drug absorption, <sup>12–15</sup> and retrosynthetic techniques assist with route selection. <sup>16–19</sup> Crystal structure prediction (CSP) and solubility predictions are also increasingly being adopted.<sup>20-26</sup>

The paths envisaged to digitally design a drug product are depicted in Figure 1. The difficulty lies in the interrelation of the many complex pathways, with the selection of the crystal

Received: November 21, 2023 Revised: June 3, 2024 Accepted: June 4, 2024

Published: June 24, 2024





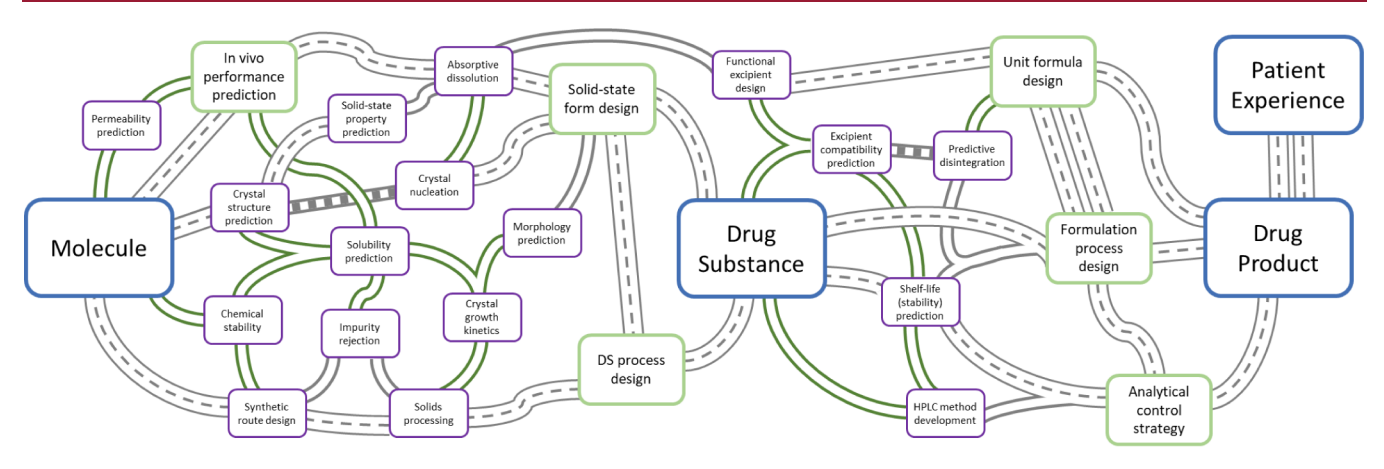


**Figure 1.** Conceptual roadmap illustrating the complex network of major elements (in bold) and associated work streams necessary for developing a new molecular entity into a solid oral drug product. The grading of the roads is an estimate of how well the two end points are connected (DS stands for drug substance, the active pharmaceutical ingredient contained in the finished dosage form of the drug product).

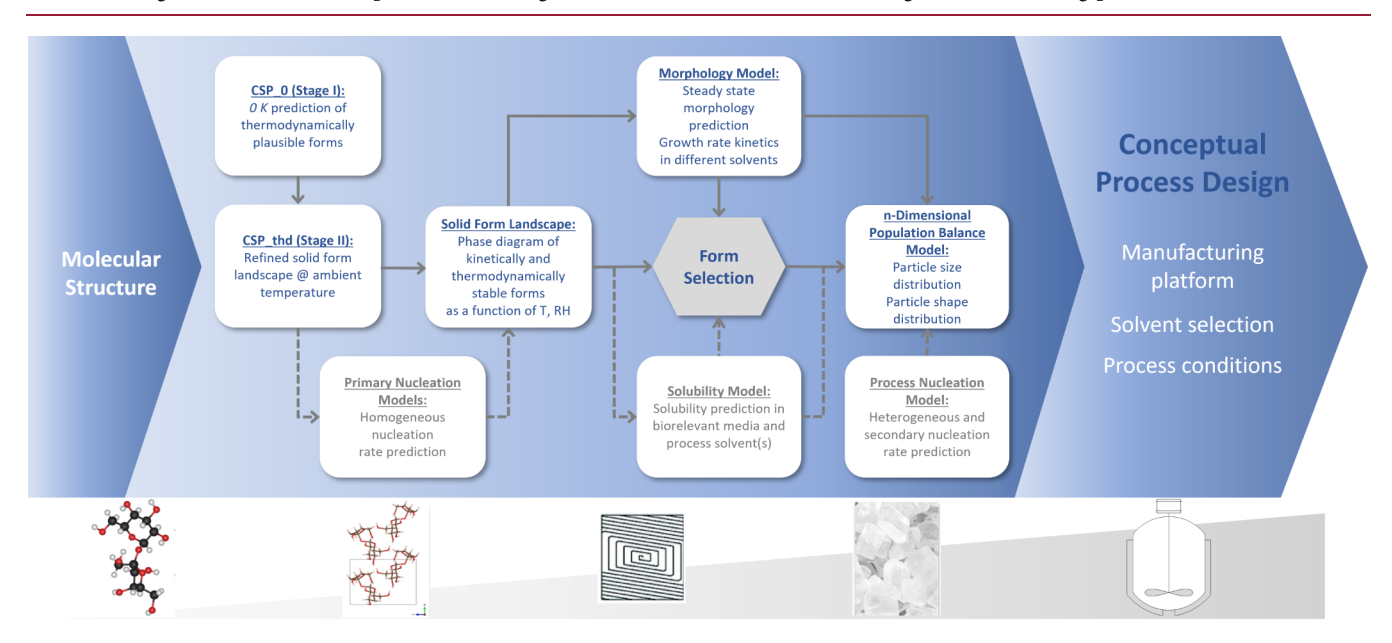


**Figure 2.** Schematic digital workflow to define a conceptual crystallization process, starting from a molecular structure on the left and proceeding to the crystallizer on the right. Ab initio models discussed in this paper are depicted in blue; those for which first-principles models are not yet sufficiently accurate (currently determined experimentally) are colored gray.

form in the solid oral dosage being the most critical — if this changes, most of the process must be repeated, particularly clinical trials which test whether the new form is equivalent to any previously tested in humans.

A recent review<sup>27</sup> summarized the emergence over the last two decades<sup>28–30</sup> of the concept of digital design and the use of computer modeling to complement experimentation for the design of solid forms and their crystallization processes. Progress in many steps has been assessed, from the blind tests of crystal structure prediction organized by the Cambridge Crystallographic Data Centre (CCDC)<sup>31</sup> and the aqueous solubility prediction challenges,<sup>32</sup> to Faraday Discussion meetings on crystallization,<sup>33</sup> as well as the output of the crystallization working group of the Enabling Technologies Consortium.<sup>30,34</sup>

This contribution evaluates how current computational tools can be combined in a workflow to design crystallization processes starting from the molecular structure of the API. It is intended as a **demonstration** of the use of ab initio computational tools in the development cycle of a pharmaceutical product through the integration of the current state of the art in selecting the desired solid-state form of the API through calculation of the requisite physical properties necessary for optimal bioavailability and downstream processability. Inevitably, most computational models are more suited to certain types of molecules, and the range of molecules to which they have been successfully applied varies. This integrated computational project leads to the identification of the limitations of current physics-based ab initio methods as well as the open problems, both for each step and overall, toward developing a digital design strategy for a wide range of pharmaceuticals.

We outline the fundamental physical basis of predicting each property and illustrate these calculations for two systems, olanzapine, an atypical antipsychotic agent originally marketed by Lilly as Zyprexa,<sup>35</sup> and succinic acid. Both are small molecules compared to current small molecule APIs under development. Consideration is given to both pure computation

of absolute or relative properties and where the input of some experimental data into the simulation can provide a wide range of data with the required accuracy.

# 2. THE VISION OF AB INITIO CRYSTALLIZATION PROCESS DESIGN

Most drugs are developed as solid dosage forms, such as tablets or capsules, <sup>36</sup> due to patient preference. In silico modeling should therefore assess the entire pathway of developing an API into a new solid oral dosage form, while minimizing the risk of downstream failures. The goal is to use the ab initio results to direct the experimental effort to optimize the use of materials and resources for successful drug development. In this context, we use the term "ab initio" to mean that no experimental information about the specific compound is used.

Drug development generally progresses along two streams: the production of the drug substance and the production of the final dosage form. They are not mutually exclusive, since the drug product (containing a drug substance with the desired attributes of size, shape, etc.) must accommodate the physical properties (density, powder flowability, etc.) of the drug substance. As a result, a coordinated effort is required to achieve the best in vivo performance of the solid oral dosage form. The choice of the crystalline form of the API must meet the needs of both drug substance and drug product development and should be decided prior to or in conjunction with the synthetic route selection before other key activities can commence. Thus, the proposed digital workflow depicted in Figure 2 starts from the molecular structure with prediction of the static crystal structure landscape (CSP 0) to identify low-energy structures that are plausible polymorphs. These structures are then refined through the determination of the free energy at room temperature to allow prediction of phase diagrams (as a function of temperature, relative humidity (RH), and sometimes pressure) as well as modeling and prediction of key properties (solubility, etc.) to support the selection of the solid form.

With the desired crystal form selected, conceptual models already exist to design crystallization processes, but all require experimental data (solubility, growth rates, nucleation rates, etc.) to be available. For example, one such model estimates the fate and purge of impurities after crystallization.<sup>37,38</sup>

Our proposed digital workflow computes polymorph-specific and facet-specific growth rates for putative polymorphs and uses them to predict the crystal shape and provide insight into the process design. We employ state-of-the-art multidimensional population balance modeling to predict particle size and shape distributions, but they can only be predicted for seeded batch processes, where primary and secondary nucleation is minimized. While reliable empirical models for secondary nucleation exist, they require several material- and crystallizer-specific parameters, which must be experimentally determined. Thus, without a means to predict secondary nucleation kinetics from a first-principles approach (see Section 6), the fully ab initio conceptual design of a continuous crystallization process<sup>39</sup> is not yet possible.

## 3. CRYSTAL POLYMORPH SELECTION

The expensive and very public recall of Norvir due to the sudden appearance of a new, more stable polymorph of the API<sup>40-43</sup> prompted many, if not all, large pharmaceutical companies to make major investments in solid form and salt

screening. Selection of the solid form starts with screening of the parent compound and, if needed, is followed by identifying and screening other viable solid compositions from potentially many salts (if ionizable), cocrystals, or solvates. Hopefully, a commercially viable crystal form will emerge among the crystalline "hits". In reality, the lack of supply of the drug substance and time available for screening cause this process to be carried out iteratively at different stages of development. This creates the problem of having to repeat work if a new, more desirable form is identified late in the process. As form selection is often conducted before there is any certainty that the compound will progress further than phase I clinical trials, 44 the need to get the crystal form right must be balanced with the cost of exhaustively screening (if API supplies permit) a possibly large portfolio of molecules in this stage of development. It is thus imperative that industry-standard screens at least find the thermodynamically stable form early. 45,46 Although the industry has adopted several "best practices", the path to a commercially viable crystal form remains unpredictable and molecule-dependent; there is no one-size-fits-all protocol for crystallizing a molecule for the first time, let alone selecting a suitable solid form for a commercial drug product. This is where the in silico design of solid forms, starting with the prediction of the crystal structure, has the potential to change the game for solid oral dosage form development.

**3.1. Crystal Structure Prediction.** As a complement to the experimental screening and characterization of solid forms, <sup>47</sup> a CSP study can provide confidence that the most stable form is known, which gives assurance that a new, more stable form will not appear and potentially lead to the "disappearance" of the form under development. CSP will then allow experimentalists to right-size the search for possible crystal forms (i.e., the polymorphs of the neat API<sup>48</sup> and at least its hydrates<sup>49</sup>).

The ideal CSP code would predict all polymorphs that could be experimentally realized and give a recipe for obtaining each. The blind tests of CSP organized by the CCDC<sup>31</sup> show that this aspiration<sup>50</sup> is not yet achieved. Currently, the first stage in a typical CSP,<sup>20</sup> referred to as CSP 0, is the search for structures that are the most stable minima in the lattice energy. This is the energy required to separate a (hypothetical) static infinite perfect crystal into infinitely separated molecules in their lowest energy conformation, approximating the relative stability at 0 K. However, the relative stability of polymorphs often changes with temperature and pressure, so calculating a crystal energy landscape under processing and storage conditions (referred to as CSP thd) is needed. Other factors should also be considered, such as the particle size effect (a balance of bulk and surface energies)<sup>51</sup> which may lead to different polymorphs in confined crystallization experiments,<sup>52</sup> or environmental factors, such as water activity (or relative humidity), so that anhydrates and hydrates of different stoichiometries can be compared on the same energy landscape. 53 Furthermore, the CSP 0 landscape is dominated by unobserved structures, 54,55 which could be disorder components of observed polymorphs, but are more likely subject to facile transformations to other structures once temperature effects are considered.

3.1.1. Lattice Energy CSP. CSP studies are generally limited to a specified number of crystallographically independent molecules (often just Z'=1 and 2) and range of space groups (particularly restricted for a chiral compound). Molecular

HO OH 
$$H_3C-N$$
  $N$   $H$ 

Figure 3. Left: the molecular diagram of succinic acid, middle: the molecular diagram of olanzapine, and right: the dispersion bound dimer proposed as the growth unit of most olanzapine crystal structures. Hydrogen atoms are omitted for clarity.

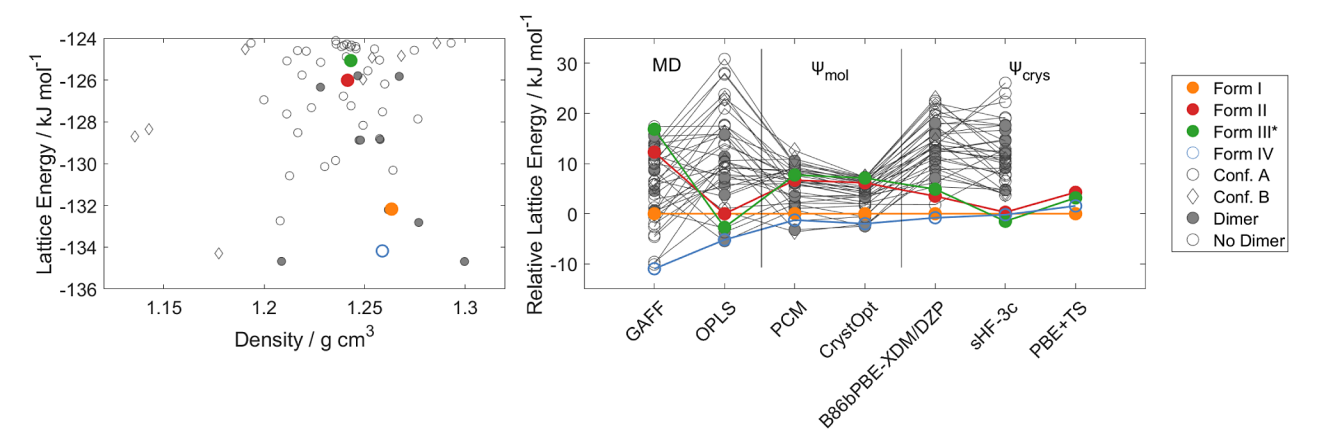


Figure 4. Left: the lattice energy landscape obtained in a  $\psi_{mol}$  CSP study of olanzapine using CrystalOptimizer (CrystOpt) for the final lattice energy refinement, <sup>59</sup> with each point representing the lattice energy and density of a mechanically stable CSP\_0-generated structure. Right: comparison of lattice energies obtained by using different energy models to optimize the structures. Conformers A and B and full references to the different computational models are given in Figure S1 and Section S1.1.1.1.

connectivity is also fixed, although in some calculations it is possible for proton transfer to occur, for example changing a cocrystal to a salt.<sup>56</sup> The stoichiometry of multicomponent forms is fixed, although the relative energies of multiple studies with variable composition can be compared. The CSP\_0 method relies on cancellation of errors to find relative lattice energies, and this means that direct comparison of different compositions is more prone to error because of the different types of molecules and intermolecular interactions.<sup>53</sup>

A CSP search must also consider the range of conformations that could plausibly be of sufficiently low energy to appear in a crystal structure. Many thousands, even millions, of structures are generated for a pharmaceutical API with only one molecule in the asymmetric unit cell (Z'=1), and far more are required for higher Z' or multicomponent systems. This necessitates a hierarchical approach to evaluating the lattice energy, with a reduction in the number of structures being evaluated using more computationally demanding methods (Section S1). Even then, many more structures will be predicted than ever realized experimentally as polymorphs.

3.1.2. Pilot Compound Results – Succinic Acid and Olanzapine. A workflow for reducing the lattice energy landscape was developed<sup>57</sup> using a recent CSP on succinic acid (Figure 3),<sup>58</sup> which was carried out following the serendipitous discovery of a new polymorph. With GAFF, over 100 CSP\_0 structures were reduced to 27 low-energy, persistent crystal structures. This work also helped to identify the types of disorder and stacking faults that probably occur in real crystal structures, particularly in the high-temperature  $\alpha$  form.

Olanzapine (Figure 3) is a good illustration of how CSP and molecular modeling may be used as complementary techniques in understanding the experimental solid-form landscape. The marketed form, form I, is the most thermodynamically stable form, <sup>35</sup> and forms II and III are only found concomitantly (usually with form I) by desolvating solvates. <sup>59</sup> There is as yet no definitive structure for form III, and the proposed match from the CSP is denoted as form III\*. The recently discovered form IV, crystallized in a polymer dispersion, does not contain the ubiquitous dispersion-bound dimer. <sup>60</sup>

Figure 4 shows that the relative lattice energies of known and CSP-generated structures of olanzapine are sensitive to the computational model used. Only when the B86bPBE-XDM/DZP optimized CSP\_0 structures were reranked with expensive single point plane-wave basis set  $\psi_{\rm crys}$  calculations, fidd the four known polymorphs become the most stable structures, all within 5 kJ mol<sup>-1</sup> of the observed most stable form I, and with form III\* the least stable.

Reducing this lattice energy landscape using our workflow<sup>57</sup> (full details are given in Section S1.1.1) gives the landscapes shown in Figure 5. This shows that the choice of force field is important since form III\* melts with GAFF, but OPLS provides a better agreement of lattice energy with the more accurate models in Figure 4. Nevertheless, most dimeric and nondimeric structures are stable, and so the explanation for form IV (which does not contain the dispersion-bound dimer) being so elusive is presumably that dimers form early in the crystallization process. Only recently, studies of the growth of an olanzapine solvate from solution have shown why the

Crystal Growth & Design pubs.acs.org/crystal Article

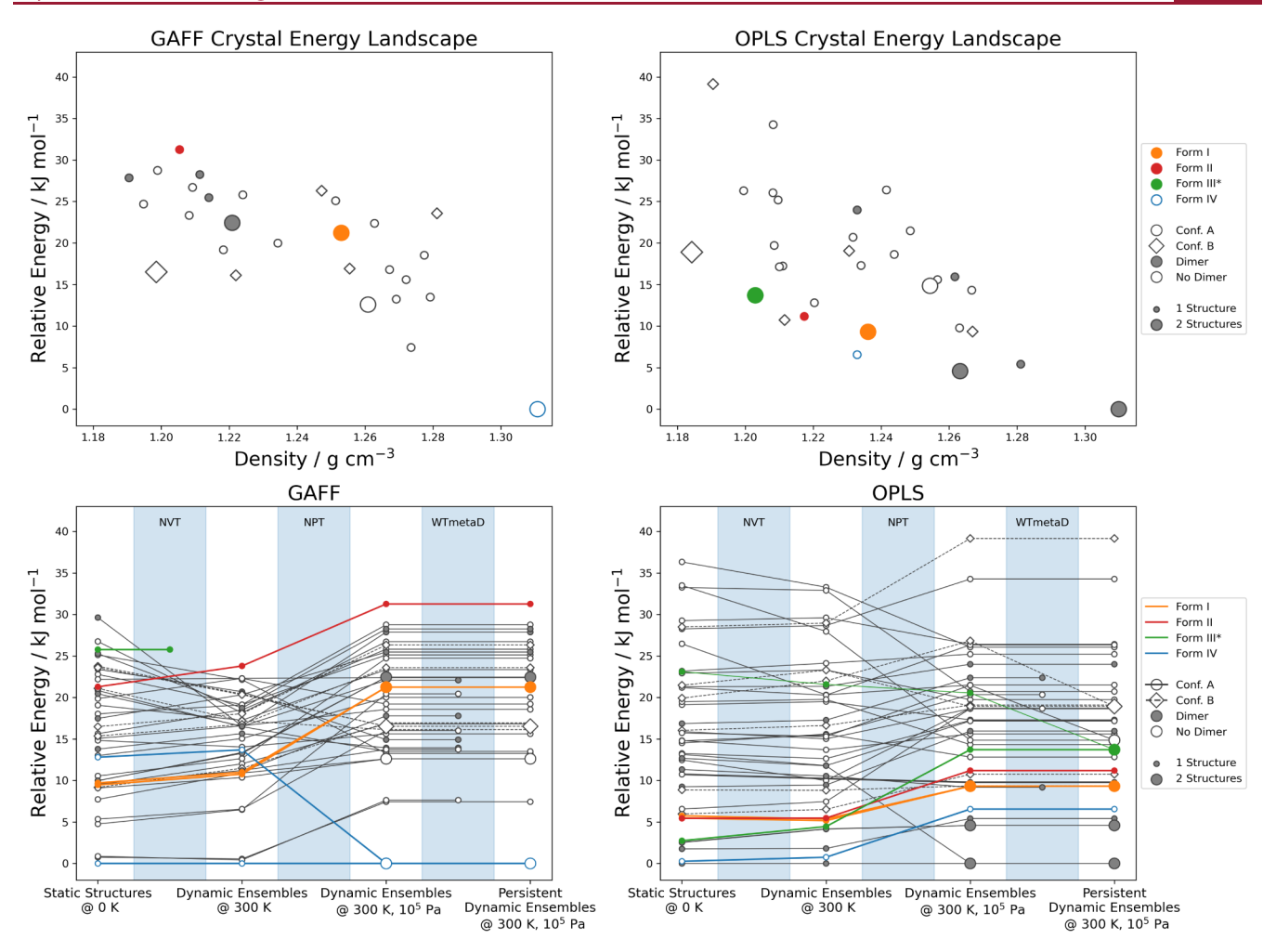


**Figure 5.** Top: The reduced energy landscapes of olanzapine: calculated with (left) GAFF and (right) OPLS, with the size of the symbol representing the number of CSP\_0 structures that have merged to that form. Bottom: the loss of structures resulting from using (left) GAFF and (right) OPLS through the clustering and WTmetaD steps. Full details are given in Section S1.1.1.2.

dimers appear to be the growth unit as often assumed,  $^{62-64}$  and this mechanism appears to be disrupted by the presence of a polymer.

The reduction of the energy landscape for olanzapine is not as extensive as for urea, succinic acid, <sup>57</sup> or ibuprofen. <sup>65</sup> While noting that the reduction extent can indeed be system-dependent, we also note that in the case of olanzapine we had preselected a subset of low-energy structures that seemed likely to be long lived. The reduction of a CSP\_0 landscape, using the observation that the number of CSP structures is reduced by an MD shakeup <sup>66</sup> and that hypothetical structures will melt, <sup>67</sup> is a major step forward to reduce the number of structures that need to be considered for more accurate calculations. Other methods are emerging that can use an estimate of the energy barriers between the different forms. <sup>68</sup>

**3.2. Free Energies of Polymorphs.** The relative stability of many polymorphs can change with temperature, with as many as 21% of polymorphic pairs exhibiting an enantiotropic relationship. Hence, it is important to go beyond the 0 K lattice energies and calculate relative free energies (CSD\_thd). Relative free energies of polymorphs differ from relative 0 K lattice energies because of the variation in the vibrational modes and frequencies between polymorphs. There is also a mixing of the intermolecular and intramolecular modes for

flexible molecules,<sup>70</sup> and some motions are so anharmonic that they can be observed as dynamic disorder.

3.2.1. Ab Initio Free Energies in the Harmonic Approximation and beyond. The harmonic approximation can be used in periodic density functional codes with an increasing range of density functionals and dispersion interactions<sup>71</sup> to determine the phonons and hence lattice free energies. As different polymorphs usually have very different unit cells, care must be taken to use a sufficiently large supercell for comparisons (i.e., converge the Brillouin zone).

Free energies can also be calculated using biased molecular dynamics,  $^{72-74}$  which is discussed further in Section S2.1. The use of a reference model system, namely the Einstein crystal,  $^{75-77}$  coupled with free energy perturbation (FEP) or thermodynamic integration (TI),  $^{78}$  provides an alternative method. These methods and some of their modifications have been implemented in MD packages.  $^{79-82}$  Some inherent errors in calculating relative free energies are removed by using the Lattice Switch Monte Carlo (LSMC)  $^{83}$  method, which has mainly been used in atomic solids.  $^{83-85}$  A further enhancement using the exact Zwanzig-Bennett relationship shows promise.  $^{86-90}$  Application to carbamazepine demonstrated precision at a level of  $\pm 0.01$  kcal mol $^{-1}$  ( $\pm 0.04$  kJ mol $^{-1}$ ) in computed free energy differences with just 5 ns of computing time per

polymorph pair. <sup>90</sup> All of these methods are described in greater detail in Sections S2 and S3.

Directly calculating free energy differences between polymorphs via MD by simulating phase transitions requires augmentation by suitable enhanced sampling methods. 73,74 Methods include static biasing approaches, such as umbrella sampling (US), 91,92 as well as history-dependent biasing methods, such as metadynamics (MetaD). 93-95 Both assume the ability to sample reversibly a pathway between different crystal forms and to represent such a pathway in a lowdimensional set of collective variables (CVs). Static approaches require some a priori knowledge of the transformation pathway between crystal forms, and combining a series of simulations connecting the metastable states (polymorphs) of interest enables the calculation of global free energy surfaces and, in turn, free energy differences. 91,92,96,97 History-dependent methods can explore low-dimensional CV spaces to autonomously identify transition pathways. In MetaD, the bias potential discourages the visitation of previously sampled configurations, leading to exploration of unseen configurations and the discovery of transition pathways connecting metastable states. The adaptively constructed total bias can be rigorously removed to give the unbiased probability and, hence, the free energy of metastable states.  $^{98-102}$ 

Another approach via direct MD sampling builds on the adiabatic free energy dynamics (AFED) methods developed by Rosso and Tuckerman. Crystal-AFED is a variant of the driven-AFED algorithm, where CVs are adiabatically decoupled from fast degrees of freedom and sampled at an artificially high temperature.

3.2.2. Pilot Compound Results – Succinic Acid and Olanzapine. For succinic acid, calculating the Helmholtz free energy using harmonic phonons stabilizes  $\beta$  succinic acid such that it is more stable than  $\gamma$  succinic acid at ambient temperatures, although the energy differences are minimal. An alternative proposed framework for the thermodynamics of polymorphs uses ab initio Gibbs free energy calculations based on machine-learned potentials, including a path integral quantum nuclei correction, and correctly predicts that  $\alpha$  is the high-temperature form.

Recently, a limited CSP\_thd study of olanzapine, using embedded fragment quantum mechanical methods, <sup>109</sup> compared the calculated frequencies of the two most stable structures (forms I and II) with experiments and confirmed that form I was monotropically more stable than form II. An alternative method <sup>110</sup> gave the same stability order for lattice energies as the PBE-TS calculations shown in Figure 4, but showed that forms IV and III swapped stability order at around 200 K.

**3.3.** Open Problems in CSP and Free Energy Calculations. While our understanding of the relative thermodynamic stability of polymorphs is improving, we are a long way from understanding the kinetic competition between polymorphs. Our original goal of ascertaining which solid forms are predicted to be stable under manufacturing, processing, and storage conditions remains an open question. Modeling of nucleation and growth kinetics is advancing, 111 but kinetics of transformation is limited by the available experimental information against which modeling can be benchmarked. Kinetic barriers inhibit direct observation of phase transformations. 112 The stability order of polymorphs can change only when the lattice energy difference is sufficiently small, comparable to the relative thermal or

pressure contributions to free energy. Hence, our ability to predict phase changes is limited by the error in the relative lattice energies, which, as Figure 4 shows, is still substantial, particularly with the potential energy surfaces (force fields) that can be used to reduce the energy landscape by simulating anharmonic effects, i.e., realistic molecular movement, including thermal expansion.

CSP can play a significant role as a complement to solid form screening. There are often "predicted" structures that are competitive with or more stable than the known forms, raising the question of which unknown structures could be observed as relevant polymorphs. Calculations of lattice enthalpy as a function of pressure, anisotropy of the diamagnetic susceptibility tensor, and other physical properties of the CSP-generated structure try. Comparison of CSP-generated structures between landscapes of related molecules can also suggest crystalline templates, which have been successfully deployed in the search for catemeric carbamazepine and tolfenamic acid forms VI and VII.

The methods available for free energies require further development. The harmonic approximation is limited and does not model thermal expansion. Quasi-harmonic calculations on the thermal expansion of carbamazepine form III<sup>122</sup> show that the harmonic approximation gave errors of 1–2 kJ mol<sup>-1</sup> in both the enthalpy and entropy, which largely cancel. Pragmatic quasi-harmonic electronic structure approaches that may be applied affordably to organic crystals have been explored. There are cases where the lattice frequencies show an instability, and the entropy from the highly anharmonic motions stabilizes a high-temperature structure; methods of modeling this have been developed on metals. <sup>124</sup>, <sup>125</sup>

Estimating free energy differences usually relies on the identification and efficient computation of appropriate CVs, which is increasingly problematic with more complex growth units. This currently impacts the applicability to large-scale CSP\_thd studies with hundreds of radically different crystal forms.

## 4. SOLUBILITY DETERMINATION

The development of an industrial crystallization process requires the determination of the solubility of the API in the process solvent(s). Measuring this experimentally for the stable polymorph may be straightforward, but metastable polymorphs tend to transform into more stable forms during the experiment. <sup>134</sup>

**4.1. Methods Based on Coexistence.** The solubility can be determined by considering when the solute and solvent are in equilibrium, and so direct coexistence simulations bypass the need for free energy calculations. They involve an isobaric isothermal simulation of the crystalline solid and solution in contact. Errors can occur due to long time scale processes, such as attachment and detachment at kinks, 135,136 1D nucleation of kinks, <sup>137–139</sup> and 2D island or pit nucleation. <sup>140–145</sup> Special "everkinked" crystal orientations can eliminate these nucleation phenomena, 142,146 and enhanced sampling methods allow better estimation of the attachment and detachment rates at kink sites, as recently demonstrated for organic molecules 147 and salts. 148 However, direct coexistence only estimates equilibrium concentrations and does not estimate the chemical potential differences at nonequilibrium conditions, such as supersaturation, which drives crystallization.

## 4.2. Methods Based on Thermodynamic Integration.

Figure 6 shows an alternative route for calculating the solubility via the thermodynamic cycle and thermodynamic integration (TI). We have already seen (Section 3.2.1) how Frenkel–Ladd methods (TI for solids) can compute the free energies of solid phases. <sup>149,150</sup> An analogous TI method can provide the free energy of molecules in solution using the centroid reference of Khanna et al. <sup>149</sup> This one extra step of converting the centroid reference to the molecule provides the absolute free energy for fully anharmonic and multiconformer gas phase molecules.

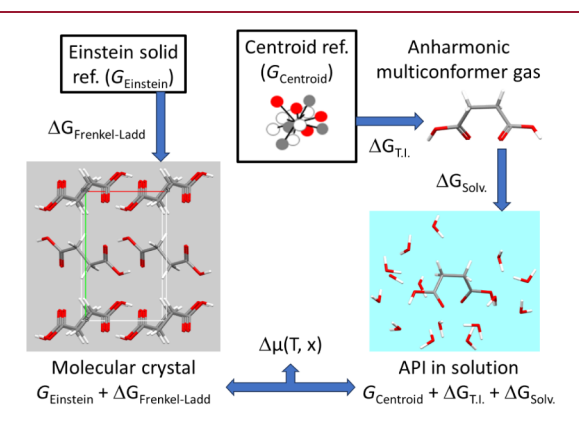


Figure 6. Thermodynamic integration starting from two reference models is used to obtain the free energy of the crystal and that of the molecules in solution. These solubility calculations are illustrated for the  $\beta$  form of succinic acid. <sup>58</sup>

The solubility can be computed by equating the chemical potential of the compound in the crystal phase with that in the solution phase, i.e.,  $\mu_{\text{crystal}}(T) = \mu_{\text{solution}}(T, x)$  where x is the mole fraction of solute in solution. The equality of chemical potentials is satisfied for the particular composition  $x_{\text{sat}}$  i.e., the solubility. Shown in Figure 7 is the chemical potential

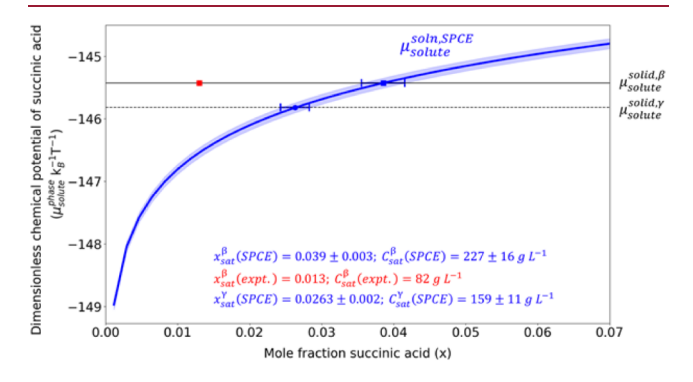


Figure 7. Chemical potential as a function of solubility mole fraction in aqueous solution at 300 K and 1 atm pressure (adapted from Figure 9 in Khanna et al.,  $^{150}$  reprinted by permission of the publisher (Taylor and Francis Ltd., http://www.tandfonline.com.), along with computed chemical potentials of the  $\beta$  and  $\gamma$  succinic acid polymorphs. The force field model used for succinic acid is GAFF, and that used for water is SPCE.  $^{151}$  The computed saturation solubility,  $x_{\rm sat}$ , of each polymorph, lies at  $\mu_{\rm crystal}(T) = \mu_{\rm solution}(T, x)$ , where the chemical potential of the compound in the crystal phase and that in the solution phase intersect. The width of the curve represents plus and minus one standard deviation in the predicted chemical potential, i.e., the "error bar" from the precision of the calculations and not the force field inaccuracy.

computed for succinic acid as a function of solution phase mole fraction at 300 K, along with the computed chemical potentials for the  $\beta$  and  $\gamma$  polymorphs. Repeating these calculations at various temperatures provides the information needed to create the van't Hoff solubility plot shown in Figure 8.

Article

4.2.1. Heat of Sublimation. The thermodynamic cycle shown in Figure 6 can be used to calculate solubility by using other, often simpler models for the heat of sublimation and the solvation energy and combining them. The heat of sublimation, the energy difference between the crystal and gas phases, is usually the best experimental test of the energy scale of the intermolecular interactions within the crystal and, hence, the lattice energy (i.e., ignoring various contributions that are of the order of 2RT for small rigid molecules). Computationally, we can better estimate the heat of sublimation from the slope of Clausius—Clapeyron plots, 150 constructed from vapor pressures calculated at each temperature by equating the chemical potential of the crystal phase with that of the gas phase, 150 as described in Section S4.

4.2.2. Solvation Energies. Calculating the solvation free energy, i.e., the work required to insert one solute molecule into the given solvent, may be problematic. Direct insertion of solute molecules into a dense solvent phase (Widom's method)<sup>152</sup> will be difficult, and so new strategies have been developed, such as Configuration Bias Monte Carlo<sup>153</sup> (CBMC) and Continuous Fractional Monte Carlo<sup>154</sup> (CFMC) methods.

Other methods use an external repulsive potential (Weeks-Chandler-Anderson (WCA) potential or Born potential) to create a cavity for solute insertion and have been used to calculate absolute solvation free energies of small neutral molecules in various solvents. 156 Mobley and Guthrie computed the free energy of hydration using explicit and implicit solvent models for nearly 650 molecules. 157 Solvation free energies of sparingly soluble solutes in different solvents have also been reported. Recently, Khanna et al. proposed a decoupling approach, combining a shorter thermodynamic cycle without solute-solvent interactions and the subsequent introduction of the Lennard-Jones and Coulombic interactions separately to compute the solvation free energy in each solvent. 158 These last two methods are compatible with popular open-source MD engines, such as LAMMPS and GROMACS.

4.2.3. Pilot Compound Results – Succinic Acid. The approach outlined in Figure 6 and in the literature 149,158 has been used to predict the solid–vapor and solid–solution equilibria of  $\beta$ - and  $\gamma$ -succinic acid at various temperatures, along with the chemical potential difference in the solution and crystalline phases. This gives the solubility plot shown in Figure 8 (the complete derivation is included in Section S4). All of the simulation points on the Clausius–Clapeyron plot (Figure S5) lie almost perfectly on a straight line, the slope of which gives the sublimation enthalpy, which is in reasonable agreement with the range of experimental values.

Polymorph stability is demonstrated in Figure 7, where the chemical potential of the  $\gamma$  crystalline form of succinic acid is lower (more negative) than that for the  $\beta$  form, indicating a more stable, less soluble  $\gamma$  solid form at 300 K and 1 atm. However, the two forms differ in their chemical potential by only  $\sim 0.4~k_{\rm B}T$  molecule<sup>-1</sup>, which is small compared to the absolute scale of  $\sim -145~k_{\rm B}T$  molecule<sup>-1</sup>. We conclude that the two forms are so close in stability that it may be

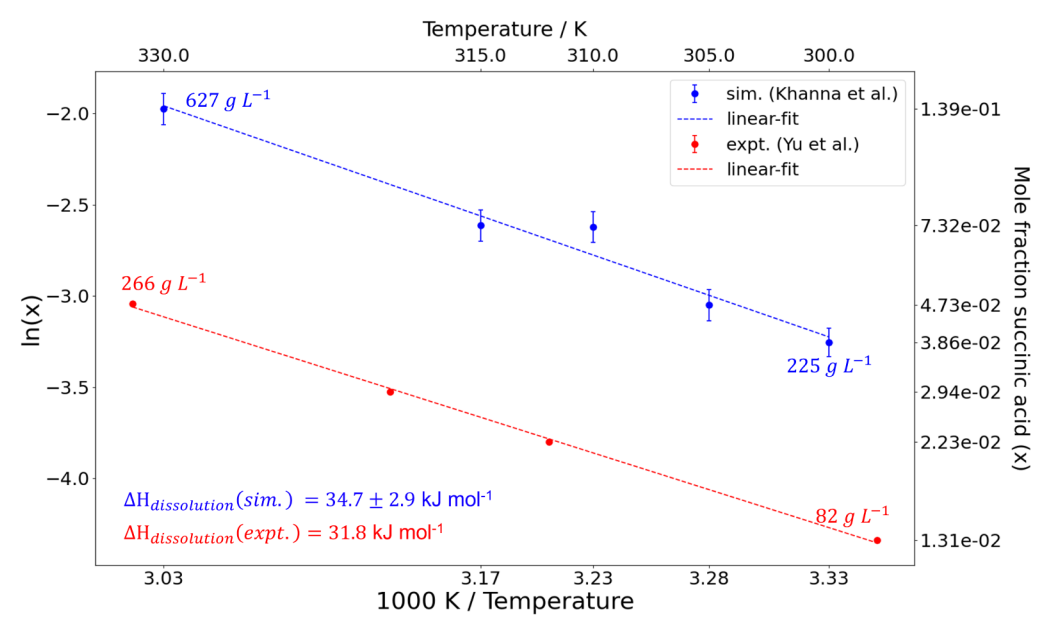


**Figure 8.** Van't Hoff solubility plot for  $\beta$  succinic acid in aqueous solution at atmospheric pressure. Experimental data points are taken from Yu et al. 159 and simulation data points from Khanna et al. 150 Adapted from Figure 11 in Khanna et al., 150 reprinted by permission of the publisher (Taylor and Francis Ltd., http://www.tandfonline.com).

challenging to rank order them, as also shown by the relative lattice (Section 3.1.2) and free energies (Section 3.2.2). However, verifying this experimentally will first require an experimental protocol for producing and isolating the elusive  $\gamma$  form, which has only been observed once in the lab as a concomitant solid with the commonly observed  $\beta$  form. Section 18.

Harmonic phonons have also been used within the thermodynamic cycle to calculate the solubility. Using the  $\psi_{\rm mol}$  estimate of lattice energies (Section 3.1.1) with the harmonic phonons (Section 3.2.1) for the heat of sublimation and a well calculated hydration energy can rival the accuracy of informatics models for calculating absolute solubility. 160 This study showed that using atomistic MD simulations and FEP methods with GAFF for succinic acid and SPCE for water gave a hydration energy of -57.47 kJ mol<sup>-1</sup>, in somewhat better agreement with experiment  $(-61.08 \text{ kJ mol}^{-1})^{161}$  than various implicit solvation models. A  $\psi_{mol}$  estimate of the lattice energies and thermal corrections from  $\psi_{crvs}$  harmonic phonon calculations 160 gave a heat of sublimation of 121.04 kJ mol<sup>-1</sup> (c.f. 162 of 123.2 kJ mol-1 which can be compared with the Clausius-Clapeyron plot in Figure S5), and aqueous solubility of 0.447 mol L<sup>-1</sup> (equivalent to 52.75 g L<sup>-1</sup>), more accurate than the best machine learning estimate (c.f. experimental: 70 to 82 g  $L^{-1}$ ). 160

The solubility for olanzapine was not calculated using the Einstein crystal method because the force fields were shown to inadequately represent the known polymorphs (Figure 5 shows that GAFF gives an incorrect stability order and form III\* melts).

**4.3. Open Problems in the Calculation of Solubility.** Solubility prediction is an ongoing challenge for "first-principles" methods that do not require any experimental input. The simplest strategy accounts for solvation through an implicit model, often based on Poisson—Boltzmann equations <sup>163</sup> or polarizable continuous medium models <sup>164</sup> in combination with density functional theory calculations. A related strategy used extensively in pharmaceutical crystallization is the conductor-like screening model for realistic

solvents (COSMO-RS). This uses ab initio calculations to obtain "sigma profiles" (surface charge density profiles) specific to each solute and solvent molecule. Solvation free energies are estimated via a thermodynamic cycle of melting and mixing with the solvent sigma profiles. This method is based on solvation thermodynamics and can benefit from the growing open-source database of "sigma profiles" for different solvents. 165 Although the COSMO-RS approach offers a route to exploring both single solvents and mixed solvents (especially solvent-antisolvent mixtures) into crystal growth and morphology modeling, there is a limitation of the requirement of experimental melting data for the drug crystals that may not be obtainable when there is thermal degradation. The method is also not congruent with fully ab initio predictions of solubility. However, the COSMO-RS predictions could be refined using more reliable solubility data generated through molecular dynamic simulations, either as solubility or as the enthalpy of dissolution.

Explicit solute-solvent simulation methods also have their own challenges. Direct coexistence simulations are susceptible to undetected errors and cannot provide thermodynamic driving forces beyond the solubility limit. Methods based on thermodynamic cycles require precise free energy calculations for the crystal phase, gas phase, and solvation free energies. All three free energy calculations can now be done precisely, but accuracy remains limited, even for the best available force fields. Given the difficulty in experimentally determining the thermodynamic differences between polymorphs or even their melting points and heats of fusion, further progress in calculating solubilities is necessary and expected. Efforts to predict solubility from first principles have a significant advantage over machine learning methods, which require large, high-quality experimental data sets for training. 160 An open challenge in solubility prediction is to combine machine learning with physical principles in ways that can guide the rational selection of solvents. 166

## 5. CRYSTAL GROWTH AND MORPHOLOGY PREDICTION

Crystal morphology plays a significant role in pharmaceutical manufacturing due to the difficulties in processing needle-like and plate-like crystals. Hence, the industrial goal is to produce well-faceted prism-like crystals in the size range of 30–80  $\mu$ m. <sup>167</sup>

Crystals are usually grown in the layer-by-layer regime in order to reject impurities and obtain well-formed particles. The growth mechanism includes many steps, such as solute transport in the solution, surface adsorption, surface diffusion, and incorporation into kink sites. 168,169 Mechanistic models are often based on the assumption that the slowest process is solute incorporation 170–172 at the kink sites on step edges formed by spiral growth from screw dislocations, 170 or 2D nuclei forming on the crystal surface. 171,173-176 For spiral growth, to calculate growth rates (typically 5-100 nm s<sup>-1</sup> for API molecules) of each face, the step height and step velocity are required as well as the critical length of each side of the spiral. The critical length can be calculated using the Gibbs-Thomson equation, 1777 but the step velocity is more challenging and relies on the assumption that it is constant once the critical length is reached. 177,178 Ideal growth units and centrosymmetric growth units allow the calculation of the step velocity from the kink density, which in turn is calculated from the kink energy. The kink energy for the vapor phase may be calculated using an atom-atom force field, such as GAFF, and can be solvent-modified using solubility parameters or other approaches. 179-182

For centrosymmetric growth units, the attachment rate constant is assumed to be site-independent, and the detachment rate constant depends on the bonding structure of the site. These assumptions give a linear step velocity relationship, which has been validated experimentally. <sup>183–185</sup> The concept of periodic bond chains (PBCs) <sup>186–188</sup> describes the strongly bonded directions in the crystal, and faces that have two or more PBCs grow slowly relative to the faces with one or zero PBCs, and tend to dominate the surface structure. <sup>189</sup>

The steady-state growth shape of the crystal is determined from the Frank-Chernov construction <sup>190,191</sup> which states that the ratio of the face velocity to its perpendicular distance from an origin inside the crystal is the same for every face. Section S5 includes a fuller description of the overall mechanistic approach, depicted schematically in Figure 9, which has been applied to several molecular crystals and shows good agreement with experimental morphologies. <sup>176,182,192–195</sup>

**5.1. Pilot Compound Results** – **Succinic Acid and Olanzapine.** Succinic acid is a centrosymmetric molecule, and it has been established that the growth unit in olanzapine is the centrosymmetric dimer (Figure 3), <sup>64,196–199</sup> and so these cases can both be treated as centrosymmetric growth units. Figure 10 shows the predicted morphologies of succinic acid grown from water and olanzapine grown from ethyl acetate.

**5.2.** Growth and Morphology for High Supersaturations and Noncentrosymmetric Molecules. Kinetic Monte Carlo (kMC) simulations show that the kink density increases rapidly with supersaturation. Therefore, the equilibrium Boltzmann treatment becomes invalid at high supersaturations <sup>202,203</sup> even for centrosymmetric molecules, which is especially relevant for antisolvent crystallization. Models for the growth and morphology of noncentrosymmetric growth units have been developed for two growth units <sup>204</sup> and for any

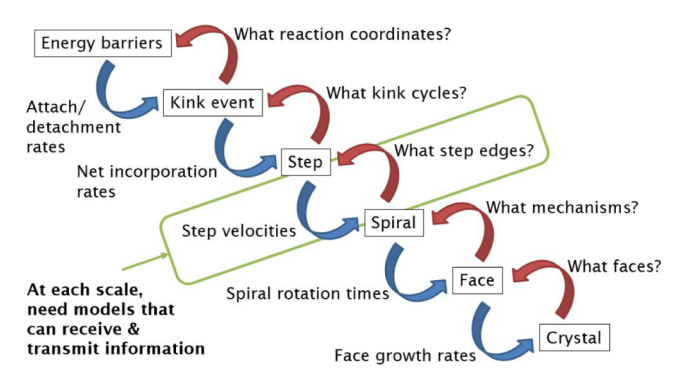


**Figure 9.** Schematic representation of the mechanistic growth model for calculating absolute growth rates of crystal faces. The red arrows indicate the questions asked during the assembly of the growth model; the blue arrows indicate the type of calculations required to execute the growth model.

number of growth units, <sup>205,206</sup> which are more complex since the arrangement of growth units differs in different growth directions. The concept of kink cycles has been developed, but the link between step velocity and kink rate/kink cycle is still not agreed upon, with many proposed relationships. <sup>205–207</sup> Good results have been produced by some expert groups, <sup>208–210</sup> and the two most advanced digital morphology aids at present are ADDICT<sup>211</sup> and CrystalGrower. <sup>212</sup>

**5.3.** Absolute Growth Rates. Molecular simulations are used to generate the free energy landscape at a given temperature and pressure for the undocked and docked growth units in the kink site. The transition path through this surface is determined to calculate the activation energy barrier, and transition state theory used to obtain a value for  $k^+$ , the attachment rate constant for growth units into kink sites. This has been used successfully for barite grown from water<sup>213</sup> and sodium chloride grown from water. The simplicity of the sodium chloride system (all major faces are identical) permitted a prediction of absolute crystal growth rate as a function of supersaturation, with the predictions being in good agreement with experiments.

The complete set of absolute growth rates can be derived from the prediction of relative growth rates coupled to one absolute growth rate, significantly reducing the computational cost. The resulting growth rates can then be used, for example, in multidimensional population balance models.<sup>215</sup>

**5.4.** Open Problems for Morphology and Growth Rate. Despite these successes, modeling methods are not quite ready for application to the everyday workflow in API research and development (but they are much closer than they were ten years ago). Open problems include:

- developing nonequilibrium kink density models (as a function of supersaturation) for crystals with many (>2) noncentrosymmetric growth units in the unit cell.
- developing step velocity models for such systems.
- improving methods for estimating solvent-modified bond energies, particularly for solvent mixtures, and especially mixtures of solvent and antisolvent.
- prediction methods for attachment rate constants for API-like solutes with multiple "floppy" functional groups. It has been shown that conformational equilibria, as well as conformational transition mechanisms, can become the kinetic bottleneck in crystal growth<sup>216</sup> and that the presence of slow conformational

Crystal Growth & Design pubs.acs.org/crystal Article

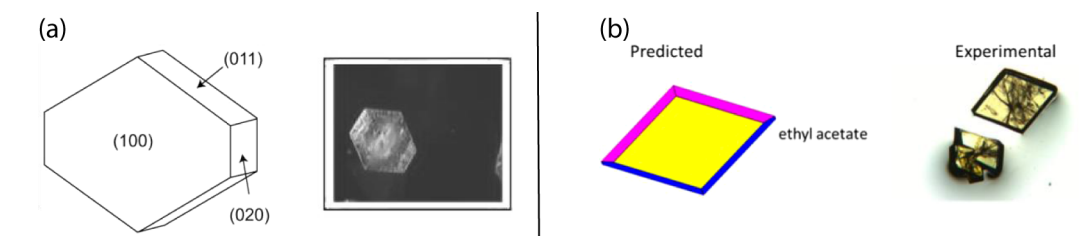


Figure 10. (a) Succinic acid crystals ( $\beta$  form) grown from water; left – predicted morphology, right – experimental shape, adapted from Figure 7 in Snyder et al., <sup>200</sup> with permission from Wiley, Copyright © 2007 American Institute of Chemical Engineers (AIChE), and (b) olanzapine crystals (Form I) grown from ethyl acetate; left – predicted morphology (yellow = (100), blue = (11–1), magenta = (011)), right – experimental shape, adapted from Figure 7 in Sun et al. <sup>201</sup>

equilibria can affect overall crystal growth rates at the process scale. How to identify molecular systems subject to these conformational limitations and how to generalize growth rate estimates in such cases remain open challenges.

## 6. NUCLEATION

Nucleation is the initial irreversible step in the formation of a new crystal. However, at industrially relevant supersaturations, nucleation is an extremely rare event and direct atomistic simulations cannot access realistic nucleation rates. One important reason for interest in nucleation is in polymorph discovery. Late-appearing polymorphs are those whose nucleation has usually been kinetically outcompeted by other polymorphs. The cases of disappearing polymorphs are likely to arise when the more stable form has a very slow nucleation rate but a fast growth rate (Table 1). In this context, atomistic simulations, while unable to provide estimates of absolute nucleation rates, could help in ranking the relative nucleation kinetics of different forms, at least in the absence of impurities, and thus provide approaches beyond thermodynamics to refine CSP-generated crystal energy landscapes and identify longlived putative polymorphs. Thus, an ability to model nucleation could allow the assessment that there is little risk of a computationally more stable crystal structure that has not been observed in extensive screening disrupting the manufacture of a metastable but kinetically favored form.

Rare event methods<sup>91,217,218</sup> make it possible to compute single-component nucleation rates under realistic conditions, even for extremely slow nucleation processes.<sup>219–222</sup> However, formidable challenges remain, especially for solute precipitate nucleation<sup>223</sup> and heterogeneous nucleation.<sup>224</sup> The challenges originate from multiple factors.

- Unlike predictions of structure and stability, which only require bulk solid properties, understanding nucleation requires a quantitative understanding of the solvent properties, <sup>223–227</sup> interfaces, <sup>228,229</sup> and perhaps also interactions with other surfaces, impurities, surfactants, etc. <sup>230,231</sup>
- Nucleation rates are highly sensitive to supersaturation.
  For quantitative comparisons and predictions, experimental and simulated supersaturations should match.
  Therefore, precise solubility and driving force calculations are important (and nontrivial) first steps.
- Nucleation is an intrinsically irreversible nonequilibrium process, and (for solute precipitate nucleation) the solid invariably has a different composition from the starting solution.
   223,234 The transformation from a solution with

- one composition to a solid with another poses tremendous difficulties for simulations.
- Most theoretical analyses and simulations focus on well-defined homogeneous primary nucleation processes.<sup>235</sup>
   However, most nucleation processes occur by heterogeneous nucleation.<sup>227,230,236,237</sup> or secondary nucleation.<sup>238,239</sup>
- 6.1. Homogeneous Nucleation. Homogeneous nucleation, in the context of API crystallization, is the spontaneous emergence of a stable (or metastable) crystalline or amorphous phase from a pure metastable solution, with no assistance from templating surfaces or particulates. In experiments, homogeneous nucleation tends to be the most difficult pathway to observe because heterogeneous or secondary nucleation pathways usually intercede. For simulations, understanding homogeneous nucleation is often the first goal because it occurs in a well-defined, pristine solution. Nevertheless, there is a significant problem in controlling the supersaturation during a simulation of solute precipitate nucleation because of the difficulty of keeping the chemical potential difference constant in a small box with a constant number of molecules.<sup>240</sup> Putting a small nucleus to seed the simulation can estimate rates without artifacts from supersaturation depletion, but this requires a priori assumptions about nucleus structure. 232,233,241,242 Osmotic ensemble methods can control supersaturation with no assumptions about the nucleus structure,<sup>243</sup> which may prove particularly useful in studies of two-step homogeneous nucleation.<sup>229,244,245</sup>
- **6.2.** Secondary Nucleation. Secondary nucleation, in multiple ways, is the opposite of homogeneous nucleation. While homogeneous nucleation involves molecular-scale spontaneous assembly from solution with no crystals present, secondary nucleation occurs by mechanical breakage of existing macroscopic crystals into preformed viable crystallites. 223,246,247 Homogeneous nucleation rarely (if ever) occurs in an industrial crystallizer. In contrast, secondary nucleation is considered to be the dominant mechanism. 238,248-250 Quantitative models have been developed for secondary nucleation, assuming that crystals can fracture on collision, accounting for crystal-crystal collisions, impeller-crystal collisions, and other mechanisms. 223,246,247,251 The solute morphology and mechanical properties<sup>252</sup> are important in determining the ease of fracture, but this is not explicit in current models, in which fracture enters through a parameter that is experimentally determined. Secondary nucleation models are extremely useful for industrial crystallization<sup>253</sup> but not for polymorph screening, where the main targets are low-energy solid forms that are predicted to be kinetically stable but are yet to be experimentally realized (Section 3.3).

**6.3. Heterogeneous Nucleation.** Heterogeneous nucleation can occur where the solution contacts a bubble, an oil droplet, or an atomically smooth solid surface. <sup>223,231,254</sup> Like homogeneous nucleation, these special cases of heterogeneous nucleation are amenable to theoretical modeling and molecular simulations. We have gained tremendous insight from these studies, e.g., how solid-crystal, solid-solution, and crystal-solution interfaces modulate nucleation barriers, <sup>230,231,237</sup> and how barriers for heterogeneous nucleation relate to barriers for homogeneous nucleation. <sup>237,255</sup> Theory and simulation have also explained how barriers are influenced by additional factors like line tension, <sup>256,257</sup> lattice mismatch/elasticity, <sup>258,259</sup> curvature, <sup>260,261</sup> hydrophobicity, <sup>262,263</sup> electrostatics, <sup>264,265</sup> and adsorbates. <sup>261,266–268</sup>

The role of heterogeneous nucleation in polymorph discovery, where another organic impurity or template crystal is involved, is discussed at greater length in Section S6.1.1.

**6.4. Open Problems in Nucleation.** We have already identified many open problems in nucleation. In most batch industrial crystallizers, nucleation can be practically avoided by seeding but the collision-induced mechanism of secondary nucleation is vital for continuous crystallizers. However, at the polymorph screening and solid form discovery phases, homogeneous and heterogeneous nucleation processes are critical. A key issue will be how much the simulation methods and analysis tools for simple systems translate to API molecules. The dominant mechanisms for conformational transformation can change significantly between the solution phase and as the molecule becomes incorporated into the crystal, even for molecules as small as ibuprofen.<sup>216</sup> An early systematic study aimed at quantifying the impact of molecular flexibility on the nucleation kinetics of four para-substituted benzoic acids suggests that conformational change is only one of the many activated processes that contribute to and control the kinetics of crystallization. Its relative weight in the whole process will change depending on the system.<sup>20</sup>

#### 7. PROCESS DESIGN

One can construct population balance models (PBMs), which can be used to predict the particle size distribution (PSD), particle shape distribution, and other important processing parameters, from known (or predicted) growth rates, solubility values, and nucleation rates (if available). The standard universal PBM, applicable to batch, semi- or fed-batch, and continuous processes, is given in Section S7.

Solubility predictions are needed to accomplish conceptual process design to drive the PBM, to determine the processing conditions, and to estimate the yield. COSMOtherm is widely used to predict solubility in any solvent from only the SMILES information. The solubility predictions are improved for a range of pure solvents or solvent mixtures when using either an experimentally measured enthalpy of fusion of the polymorph or the experimentally measured solubility of the polymorph in one or more solvents. In the absence of experimental values, the enthalpy of fusion can be estimated using quantitative structure-property relationship (QSPR) models, but this approach does not distinguish between polymorphs. To overcome this deficiency, the enthalpy of fusion can be assumed to be equal to the enthalpy of dissolution, which is estimated well by molecular simulation, as we have demonstrated for succinic acid in aqueous solution.

**7.1. Pilot Compound Results – Succinic Acid and Olanzapine.** We have performed a COSMOtherm solubility

screen in 66 solvents for both succinic acid and olanzapine (Section S7.1). The results for the  $\beta$  form of succinic acid were slightly improved using the enthalpy of dissolution determined from molecular simulation as an approximation for the enthalpy of fusion (Section S7.1 and Table S5). The results for olanzapine recommend just two candidate process solvents, ethyl acetate and methyl ethyl ketone, with no clear advantage of one over the other. Considering ethyl acetate, the conceptual crystallization process design suggests a process with 12 volumes of ethyl acetate (a ratio of 12 L of solvent to 1 kg of olanzapine) to give a dissolution temperature of 65 °C. The mixture would be heated to 70 °C, transferred through a polish filter to the crystallizer, cooled to 59 °C, to establish a relative supersaturation of 20%, and seeded. The suspension would be cooled slowly to 20 °C, filtered, washed, and dried with an expected yield of 80%. Ethyl acetate was the chosen solvent for the commercial manufacture of olanzapine. A detailed description of the virtual solubility screen along with further implications for a conceptual process is given in Section

The seeded batch crystallizer case is relevant for most drug substance crystallization processes. As illustrated, it is possible to consider the ab initio conceptual design of the batch process, provided that the solubility can be reliably predicted. Optimal cooling profiles for seeded batch crystallization were first considered by Mullin and Nývlt<sup>270</sup> and later by Ward et al. <sup>271,272</sup>

PBMs for batch crystallizers have also been used by Mazzotti and coworkers to explain the important yet mysterious phenomenon of chiral deracemization in both nature and in vitro, <sup>273</sup> i.e., where all crystals in a racemic mixture evolve to become either all *R*- or all *S*-enantiomers, known as Viedma ripening.

PBMs have been used to explain the behavior and design of continuous crystallizations, including crystallizer stability and control, and especially polymorph control. Unfortunately, the models for continuous crystallization all require secondary nucleation rates to drive them, which at present demand extensive experimental data and parameter estimation. Currently, it is not possible to predict either primary or secondary nucleation rates ab initio. As a result, the conceptual process design for continuous crystallization cannot be predicted without experimentally derived parameters.

**7.2. Open Problems in Conceptual Process Design.** Until the current inability to predict secondary nucleation from first principles is solved, there can be no further progress in the ab initio design of continuous crystallization processes. Related difficulties include the need for first-principles models for agglomeration and attrition.

Multidimensional PBMs have the potential to predict not only the particle size distribution but also the morphology (habit) distribution. However, they are not used widely because a separate growth rate model is needed for each individual facet on the crystal surface. As noted earlier in Section 5, one way to overcome these difficulties is to reformulate the multidimensional PBM in terms of a single absolute growth rate for one of the crystal faces and relative growth rates for all others.<sup>215</sup> Ab initio growth models may then be used to estimate all the growth terms in the PBM. Such an approach has never been tested but is ripe for further research.

Using COSMOtherm with QSPR to predict solubility and thus identify possible process solvents neglects the knowledge

Crystal Growth & Design pubs.acs.org/crystal Article

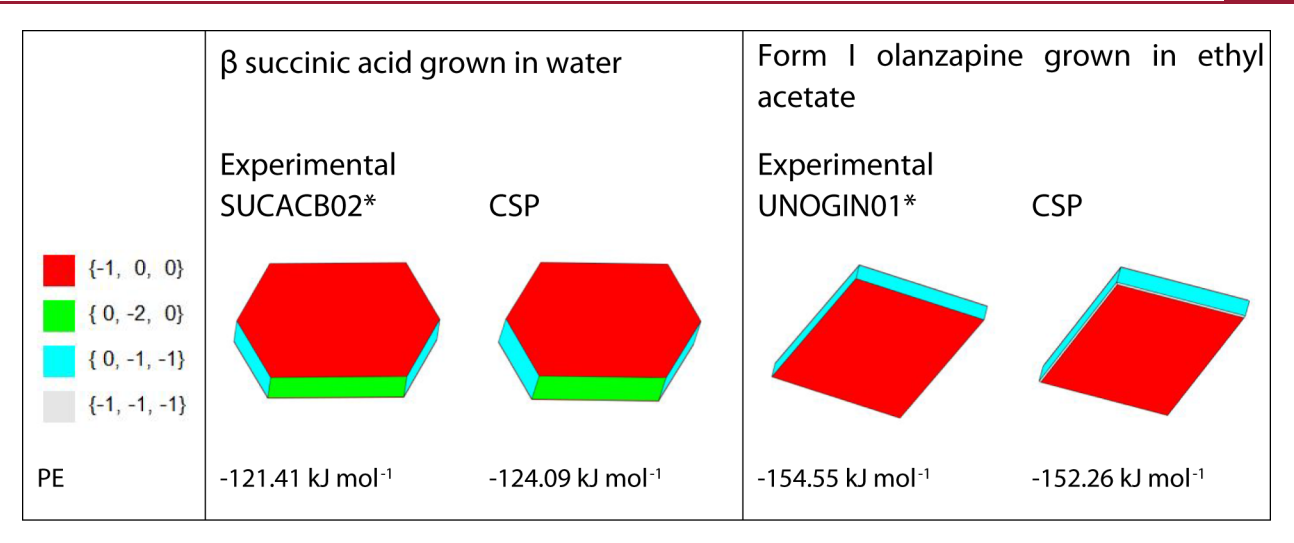


Figure 11. Comparison of morphology predictions using the CSP-generated crystal structure and experimental crystal structure. The morphologies were calculated with the CLP force field and vOCG solvent model and can be compared with other calculations and the experimental morphologies shown in Figure 10. The packing energies (PEs) calculated with the CLP force field approximate the lattice energy if conformational changes are neglected and can be compared with other estimates of the lattice energy for olanzapine shown in Figure 4 and with the heat of sublimation of β-succinic acid shown in Figure S2 if temperature effects are also neglected. The calculated relative growth rates of the crystal faces are reported in Table S5.

of the crystal form. Molecular dynamics simulations can be used to estimate solubility as a function of temperature in one or more solvents, and from that the enthalpy of dissolution may be determined. The enthalpy of dissolution can then be used, replacing the QSPR estimation for the enthalpy of fusion to improve the COSMOtherm predictions. The approach was demonstrated for succinic acid in water with limited success (see Table S5), thus the methodology needs further improvement and testing to develop a robust workflow for this concept.

As the conceptual design gets closer to industrial deployment, the influence of impurities in the solution cannot be ignored. Indeed, crystallization is the preferred means of API purification, with impurity rejection strongly impacting commercial process designs. Some impurities are not recognized by the crystal surfaces (i.e., they do not adsorb) and are inert to the growth mechanism(s). Impurities that do adsorb on crystal surfaces can significantly affect growth even at the ppm level.<sup>279</sup> Impurities normally reduce the growth rates of selected planes, thereby modifying the crystal morphology in addition to slowing down the growth process, although instances are known of impurities that accelerate growth. There is now a large literature on the effect of impurities and additives on crystal growth; selected papers include those reporting experimental methods and data and molecular models. Impurities may be structurally related to the API but with very different biological effects, so it is imperative to avoid their incorporation.  $^{291-293}$ 

Higher fidelity crystallizer models that account for imperfect mixing and other transport effects via computational fluid dynamics are available. However, they are subject to the same limitations mentioned above with respect to secondary nucleation and impurity effects.

## 8. DISCUSSION

We have shown how the components of a digital design workflow, going from the molecular structure through to the process design (Figure 2), are in an active state of development and produce worthwhile results. The time will come when this workflow can be integrated into drug discovery, allowing the discovery team to consider not only the medicinal chemistry in selecting candidates to carry forward into in vivo studies but also product and process design and the expected bioavailability of the candidate. This integration will be a game changer.

This study has illustrated that it is not fully possible for quantitatively reliable simulations to be performed prior to the synthesis and crystallization of the molecule. The main barrier is the inability to use the same energy model (e.g., force field) to predict the crystal structures and, subsequently, all the relevant properties and get sufficiently reliable results.

However, aspects of ab initio process design can be realized and useful results can be obtained for many properties. The morphology of a predicted crystal form grown from solution can be predicted, including the effect of the solvent on the relative growth rates. For example, Figure 11 shows that the predicted morphologies of succinic acid and olanzapine show little qualitative difference whether the CSP-generated crystal structure or an experimental crystal structure is used, thus demonstrating that morphology can be successfully predicted from the chemical structure. Zhang et al. demonstrated similar results for ibuprofen grown from several solvents. 298

**8.1. General Problems Identified.** 8.1.1. Crystal Structure and Temperature Effects. The most direct consequence of neglect of the temperature is neglect of thermal expansion. This can be highly anisotropic if different crystallographic directions have different strength intermolecular interactions (hydrogen bonds vs dispersion). A review of over four thousand organic crystals suggested that one-third may have at least one direction with negative thermal expansion. 299

However, the exponential dependence of many properties on the temperature is the most common limitation in the accuracy of the predicted values. The exponential dependence is a function of the ratio of the energy differences to temperature and hence makes computer modeling very sensitive to the underlying potential energy surface (force field).

8.1.2. Force Field Availability and Accuracy. A major limitation of the digital design of pharmaceutical products is the availability of sufficiently accurate force fields for pharmaceutical molecules to enable the CSP landscape reduction, free energies, morphologies, melting point, heat of fusion, and other properties to all be calculated to the accuracy required.

The sensitivity of the pharmaceutical solid state to the underlying potential energy surfaces has given considerable impetus in academia to develop more accurate energy models for pharmaceutical crystals. There is a huge effort in the theory, computer codes, and testing for both atomistic force fields (e.g., nonempirical anisotropic atom—atom intermolecular potentials combined with separated intramolecular force fields), and electronic structure calculations and fragment-based methods. Many of these emerging methods were benchmarked in the seventh blind test of crystal structure prediction. However, there are many issues, ranging from choice of functional form to selection of experimental or theoretical data for validation, which means that choice of force field will be a major factor in determining the accuracy of the simulations.

## 8.2. Polymorphism and Multicomponent Systems.

The kinetic competition between polymorphs is highly dependent on the molecule's structure. What a medicinal chemist might consider as minor differences in the molecular structure, such as introducing a methyl group or changing a hydrogen to a fluorine atom, will change the crystal structure and the propensity for polymorphism. A recent survey of 232 simply substituted chalcones ((2E)-1,3-diphenylprop-2-en-1-ones)  $^{309}$  had 170 different crystal packings, with the largest isomorphous group containing 15 compounds. Nevertheless, the digital design process could be used to foresee whether a given API was likely to be problematic to develop and whether a multicomponent form or medically similar API should be considered.

**8.3.** Utilization in Process Design. Aspects of the digital design vision of crystallization processes are currently being used for drug development. CSP is used to understand the potential form landscape and to inform and guide the experimental form selection process. Morphology predictions are used to understand and guide the effect that solvent selection can have on the resultant crystal morphology, once a crystal form has been selected.

The current state of the art of CSP, while limited by the accuracy of the potential energy surface and modeling of temperature effects, does usually identify the observed and stable polymorphs among other energetically competitive forms, as illustrated for both succinic acid<sup>58</sup> and for olanzapine (Figure 5 and refs 59 and 60). For olanzapine, as Figure 5 reveals, several forms that have not been observed experimentally are calculated to be more stable under ambient conditions than those observed experimentally. However, Figure 4 shows that either force field used to model the molecular motions gives a very different lattice energy from the most advanced electronic structure methods, where the four known forms are the most stable. The general observation that CSP usually generates more thermodynamically plausible polymorphs than are found, even in state-of-the-art industrial screening (e.g., galunisertib)<sup>310</sup> and after landscape reduction

(see Section 3.1.2), exemplifies the need for better primary nucleation models.

Table 1 illustrates the competition of nucleation and growth kinetics versus thermodynamics in predicting the form most

Table 1. Experimentally Expected Form when the Nucleation or Growth Rates of the Stable Form are Fast or Slow Relative to the Unstable Forms

stable form nucleation rate	stable form growth rate	expected form observed
fast	slow	unknown
slow	slow	unstable Form
fast	fast	stable Form
slow	fast	unknown

likely to be observed when the free energy differences between competing forms are "small". In those cases, when the more stable form exhibits faster kinetics for both nucleation and growth, it should be the form observed experimentally. Similarly, when the nucleation and growth kinetics of the thermodynamically stable form are much slower than those of the unstable form, the unstable form is more likely to be observed. Otherwise, it is unclear which form should be expected. There are cases where the most stable form has eventually been found despite being slower to nucleate and grow than the apparently stable metastable form. 311,312 However, once the solid form has been selected on the basis of experimental solid form screening with the aid of CSP, the design of the crystallization process can proceed. Provided the process is seeded to avoid primary nucleation, nucleation rates can be assumed to be negligible and thus ignored in the multidimensional PBM. This assumption enables the model to be practically used to predict the crystal size and shape distribution for a given solvent and temperature.

More reasonable expectations of state-of-the-art molecular simulation at present or in the near future are to be able to

- 1 Approximate the stability order of a set of polymorphic forms as a function of temperature.
- 2 Assess the risk of hydrate formation under real-world temperature and relative humidity conditions.
- 3 Suggest the potential for further energetically competitive polymorphs and provide their structures, which may suggest an experimental route to their discovery.
- 4 Predict the relative solubility of a given solute in different solvents.
- 5 Predict the change in solubility with respect to temperature of a given solute in a given solvent (i.e., the slope of the van't Hoff plot (Figure 8)).
- 6 Predict the morphology and the growth rates of the major facets for a set of polymorphic forms in a range of solvents.

The inability to predict the most likely crystal form to appear suggests an alternative workflow for how the current state of the art in digital design can be used for conceptual crystallization process design — to carry forward all putative polymorphs within a reasonable free energy and hence solubility range and assess the crystal morphology landscape associated with each CSP-generated form. This workflow allows for a prediction of all crystal shapes possible and allows for a priori resource and risk estimations to be made based on the complexity associated with the development of the crystallization process. For example, if only equant crystal

morphologies are predicted for all plausible polymorphs, then it can be anticipated that a smaller effort would be required to develop a crystallization process to provide a freely flowing powder. Conversely, if only needle-like crystals are predicted across all putative crystal forms, then it can be expected that more resources will be required to develop the crystalline API process to improve on the crystal morphology through the application of particle engineering techniques such as in situ milling followed by thermocycling. 313

While it is not currently possible to fully realize the ab initio vision of digital design, it is possible to benefit from the workflow provided that small amounts of experimental data are available. For example, solubility in the full range of solvents can be broadly predicted from a small set of solubility measurements, and the absolute growth rate can be estimated from knowledge of a single absolute growth rate for only one face. Both examples represent an enormous reduction in effort compared with the experimental determination of the absolute growth rates of every face on the crystal surface or measurement of solubility in thousands of solvents or solvent mixtures.

### 9. CONCLUSIONS

An industrial perspective on the engineering of pharmaceutical materials in 2007<sup>28</sup> saw computational prediction as a future step in the route from an active molecule to finished product. We have demonstrated through examples the use of simulation as part of the support to inform and guide experimental techniques foreseen in a 2015 review of the future of pharmaceutical manufacturing sciences, <sup>29</sup> and illustrated much progress in some of the opportunities identified by the crystallization working group of the Enabling Technologies Consortium.<sup>30</sup>

Computational methods are available to design a crystallization process from the chemical diagram (i.e., a priori without any experimental data) for all the main steps, apart from primary nucleation rates, which are important for polymorph discovery, and secondary nucleation rates, important for continuous crystallization process design. However, which type and level of theory are accurate enough and practically affordable is dependent on the specific API molecule, its size, conformational flexibility, functional groups, and particularly the nature of the competing polymorphs and solvates that can affect the manufacture and stability of the product. Future efforts for utilizing CSP to aid polymorph discovery and minimizing the risks of the late emergence of more stable forms should focus on primary nucleation rates. A key requirement to the implementation of the digital design workflow from the molecular diagram (Figure 2) is a priori solubility prediction, but the exponential dependence of solubility on temperature and the free energy of solution makes this a particularly challenging property to compute. Morphologies can be computed, but absolute growth rates involve challenges similar to those for absolute solubilities.

This paper shows that physics-based simulation methods are being actively developed for pharmaceuticals and are qualitatively and semiquantitatively realistic enough to be useful. As illustrated for olanzapine, the crystal structure of Form I, predicted by CSP and used to predict morphology, agrees almost identically with the experimental results without any information other than the molecular structure. Likewise, from only the molecular structure, the in silico solubility screen reduces the potential solvent systems for a thermal batch

crystallization process to less than a dozen from a field of 66 (see Section S7.1). The temperature-dependent solubility profile of the best of these, ethyl acetate (the commercially used solvent; see Figure S3), is in surprisingly remarkable agreement with experimental data of the lowest energy form. However, COSMOtherm used with QSPR has no knowledge of the crystalline form. From the temperature dependent solubility profile, a target process solvent is suggested, and a conceptual design of the crystallization process is defined.

The ideal of using the accurate potential energy surfaces for CSP and all properties and a simulation method that is realistic for the dynamics, nucleation, and growth of pharmaceutical crystals, will eventually produce more reliable quantitative multiscale modeling in the design of crystallization processes. In the meantime, such methods can considerably aid the design process by providing estimates of relative properties or uncertain parameters in approximate models (e.g., solubility). They may also be used to reduce the experimental design space and identify a small number of key experiments to conduct. As an example, once the predicted lowest energy form has been experimentally verified, the experimental crystal lattice can then be used to better predict particle morphology. Likewise, after solubility has been measured experimentally in one or more solvents, these data can be used to refine the solubility model to give better predictions of solubility in other solvents.

We have demonstrated the ab initio prediction of the crystal form landscape and solid state properties, and that process design is achievable from only the chemical structure, as exemplified for olanzapine. This workflow provides guidance of the key experiments and efforts that are necessary to move from the molecular structure to a conceptual process design, derisking the development effort. The time is near when the consideration of solid-state properties for new chemical medicinal targets will be integrated into computational chemistry approaches for the identification of new drugs.

#### ASSOCIATED CONTENT

### Supporting Information

The Supporting Information is available free of charge at https://pubs.acs.org/doi/10.1021/acs.cgd.3c01390.

Description of the hierarchical approach for energy evaluation in CSP; details of the landscape reduction of olanzapine, including further details describing Figures 4 and 5; alternative approaches to calculating free energies (biased molecular dynamics, Einstein crystal); definitions of accuracy and precision; further details of the ab initio solubility calculations; further details of morphology prediction; further comments on nucleation and simulation methods; complete derivation of the population balance model for the mixed suspension mixed product removal (MSMPR) crystallizer model; predicted solubilities for succinic acid and olanzapine in 66 solvents, and comparison with available experimental solubility information; calculated relative growth rates of faces of succinic acid and olanzapine predicted morphologies (PDF)

## AUTHOR INFORMATION

## **Corresponding Author**

Christopher L. Burcham — Lilly Research Laboratories, Eli Lilly and Company, Indianapolis, Indiana 46285, United States; orcid.org/0000-0002-1251-4725; Email: cburcham@lilly.com

### **Authors**

- Michael F. Doherty Department of Chemical Engineering, University of California Santa Barbara, Santa Barbara, California 93106, United States; orcid.org/0000-0003-3309-3082
- Baron G. Peters Department of Chemical and Biomolecular Engineering, University of Illinois Urbana—Champaign, Urbana, Illinois 61801, United States; orcid.org/0000-0003-1935-6085
- Sarah L. Price Department of Chemistry, University College London, London WC1H 0AJ, U.K.; ⊙ orcid.org/0000-0002-1230-7427
- Matteo Salvalaglio Department of Chemical Engineering, University College London, London WC1E 6BT, U.K.; oorcid.org/0000-0003-3371-2090
- Susan M. Reutzel-Edens Lilly Research Laboratories, Eli Lilly and Company, Indianapolis, Indiana 46285, United States; Present Address: SuRE Pharma Consulting, LLC, Zionsville, IN 46077; Occid.org/0000-0003-0806-5565
- Louise S. Price Department of Chemistry, University College London, London WC1H 0AJ, U.K.; ocid.org/0000-0002-7633-1987
- Ravi Kumar Reddy Addula Department of Chemical and Biomolecular Engineering, University of Illinois Urbana—Champaign, Urbana, Illinois 61801, United States
- Nicholas Francia Department of Chemical Engineering, University College London, London WC1E 6BT, U.K.; Present Address: Cambridge Crystallographic Data Centre, Cambridge, UK CB2 1EZ.; orcid.org/0000-0003-0936-2342
- Vikram Khanna Department of Chemical Engineering, University of California Santa Barbara, Santa Barbara, California 93106, United States; orcid.org/0000-0002-2918-3192
- Yongsheng Zhao Department of Chemical Engineering, University of California Santa Barbara, Santa Barbara, California 93106, United States; Present Address: OpenEye, Cadence Molecular Sciences, 9 Bisbee Ct., Santa Fe, NM 87508, USA.; ◎ orcid.org/0000-0003-1224-1787

Complete contact information is available at: https://pubs.acs.org/10.1021/acs.cgd.3c01390

#### Notes

The authors declare no competing financial interest.

#### ACKNOWLEDGMENTS

This work was funded by Eli Lilly & Company. This funding supported N.F. and partially supported L.S.P., R.K.R.A., and V.K. M.S. acknowledges support from the Crystallization in the Real World EPSRC Programme Grant (EP/R018820/1) and the ht-MATTER EPSRC Frontier Research Guarantee Grant (EP/X033139/1), which has partially supported L.S.P. We thank Dr Saurin Rawal (Lilly) for assisting with the solubility predictions from COSMOtherm. We thank Dr Rui Guo (Pfizer, formerly UCL) for providing the periodic electronic structure calculations shown in Figure 4, which were calculated via our membership of the UK's HEC Materials Chemistry Consortium, which is funded by the EPSRC (EP/X035859)

using the ARCHER2 UK National Supercomputing Service (http://www.archer2.ac.uk.)

#### REFERENCES

- (1) Deloitte. Seize the digital momentum: Measuring the return from pharmaceutical innovation 2022; Deloitte LLP, 2023. https://www2.deloitte.com/content/dam/Deloitte/uk/Documents/life-sciences-health-care/deloitte-uk-seize-digital-momentum-rd-roi-2022.pdf. accessed 08 June 2023.
- (2) The Unbearable Cost of Drug Development: Deloitte Report Shows 15% Jump in R&D to \$2.3 Billion, 2023. https://www.genengnews.com/gen-edge/the-unbearable-cost-of-drug-development-deloitte-report-shows-15-jump-in-rd-to-2-3-billion/. accessed 08 June 2023.
- (3) DiMasi, J. A.; Grabowski, H. G.; Hansen, R. W. Innovation in the pharmaceutical industry: New estimates of R&D costs. *J. Health Econ.* **2016**, *47*, 20–33.
- (4) Ooms, F. Molecular modeling and computer aided drug design. Examples of their applications in medicinal chemistry. *Curr. Med. Chem.* **2000**, 7 (2), 141–158.
- (5) Andricopulo, A. D.; Salum, L. B.; Abraham, D. J. Structure-based drug design strategies in medicinal chemistry. *Curr. Top. Med. Chem.* **2009**, 9 (9), 771–790.
- (6) Mangiatordi, G. F.; Carotti, A.; Novellino, E.; Nicolotti, O. A round trip from medicinal chemistry to predictive toxicology; Humana Press, 2016.
- (7) Abel, R.; Wang, L.; Harder, E. D.; Berne, B. J.; Friesner, R. A. Advancing Drug Discovery through Enhanced Free Energy Calculations. *Acc. Chem. Res.* **2017**, *50* (7), 1625–1632.
- (8) Kuhn, B.; Tichý, M.; Wang, L.; Robinson, S.; Martin, R. E.; Kuglstatter, A.; Benz, J.; Giroud, M.; Schirmeister, T.; Abel, R.; et al. Prospective Evaluation of Free Energy Calculations for the Prioritization of Cathepsin L Inhibitors. *J. Med. Chem.* **2017**, *60* (6), 2485–2497.
- (9) Soltani, S.; Hallaj-Nezhadi, S.; Rashidi, M. R. A comprehensive review of in silico approaches for the prediction and modulation of aldehyde oxidase-mediated drug metabolism: The current features, challenges and future perspectives. *Eur. J. Med. Chem.* **2021**, 222, 113559
- (10) Richard, A. M. Future of Toxicology-Predictive Toxicology: An Expanded View of "Chemical Toxicity". *Chem. Res. Toxicol.* **2006**, *19* (10), 1257–1262.
- (11) Valerio, L. G.; Cross, K. P. Characterization and validation of an in silico toxicology model to predict the mutagenic potential of drug impurities\*. *Toxicol. Appl. Pharmacol.* **2012**, 260 (3), 209–221.
- (12) Silverman, R. B. Chapter 2 Drug Discovery, Design, and Development. In *The Organic Chemistry of Drug Design and Drug Action*, 2 nd ed, Silverman, R. B., Ed.; Academic Press, 2004; pp. 7120.
- (13) Amidon, G. L.; Lennernäs, H.; Shah, V. P.; Crison, J. R. A Theoretical Basis for a Biopharmaceutic Drug Classification: The Correlation of in Vitro Drug Product Dissolution and in Vivo Bioavailability. *Pharm. Res.* **1995**, *12* (3), 413–420.
- (14) Oh, D.-M.; Curl, R. L.; Amidon, G. L. Estimating the Fraction Dose Absorbed from Suspensions of Poorly Soluble Compounds in Humans: A Mathematical Model. *Pharm. Res.* 1993, 10 (2), 264–270.
- (15) Yu, L. X.; Lipka, E.; Crison, J. R.; Amidon, G. L. Transport approaches to the biopharmaceutical design of oral drug delivery systems: prediction of intestinal absorption. *Adv. Drug Deliver. Rev.* **1996**, *19* (3), 359–376.
- (16) Kayala, M. A.; Baldi, P. ReactionPredictor: Prediction of Complex Chemical Reactions at the Mechanistic Level Using Machine Learning. *J. Chem. Inf. Model* **2012**, *52* (10), 2526–2540.
- (17) Liu, B.; Ramsundar, B.; Kawthekar, P.; Shi, J.; Gomes, J.; Luu Nguyen, Q.; Ho, S.; Sloane, J.; Wender, P.; Pande, V. Retrosynthetic Reaction Prediction Using Neural Sequence-to-Sequence Models. *ACS Cent. Sci.* **2017**, 3 (10), 1103–1113.
- (18) Schwaller, P.; Petraglia, R.; Zullo, V.; Nair, V. H.; Haeuselmann, R. A.; Pisoni, R.; Bekas, C.; Iuliano, A.; Laino, T. Predicting retrosynthetic pathways using transformer-based models

- and a hyper-graph exploration strategy. Chem. Sci. 2020, 11 (12), 3316-3325.
- (19) Segler, M. H. S.; Preuss, M.; Waller, M. P. Planning chemical syntheses with deep neural networks and symbolic AI. *Nature* **2018**, *555* (7698), 604–610.
- (20) Nyman, J.; Reutzel-Edens, S. M. Crystal structure prediction is changing from basic science to applied technology. *Faraday Discuss.* **2018**, *211*, 459–476.
- (21) Klamt, A. Conductor-like Screening Model for Real Solvents: A New Approach to the Quantitative Calculation of Solvation Phenomena. *J. Phys. Chem.* **1995**, *99* (7), 2224–2235.
- (22) Klamt, A.; Jonas, V.; Bürger, T.; Lohrenz, J. C. W. Refinement and Parametrization of COSMO-RS. J. Phys. Chem. A 1998, 102 (26), 5074–5085.
- (23) Vassileiou, A. D.; Robertson, M. N.; Wareham, B. G.; Soundaranathan, M.; Ottoboni, S.; Florence, A. J.; Hartwig, T.; Johnston, B. F. A unified ML framework for solubility prediction across organic solvents. *Digital Discovery* **2023**, 2 (2), 356–367.
- (24) Tung, H.-H.; Tabora, J.; Variankaval, N.; Bakken, D.; Chen, C.-C. Prediction of Pharmaceutical Solubility Via NRTL-SAC and COSMO-SAC. *J. Pharm. Sci.* **2008**, 97 (5), 1813–1820.
- (25) Lin, S.-T.; Sandler, S. I. A Priori Phase Equilibrium Prediction from a Segment Contribution Solvation Model. *Ind. Eng. Chem. Res.* **2002**, *41* (5), 899–913.
- (26) Eckert, F.; Klamt, A. Fast solvent screening via quantum chemistry: COSMO-RS approach. AIChE J. 2002, 48 (2), 369–385.
- (27) Abramov, Y. A.; Sun, G. X.; Zeng, Q. Emerging Landscape of Computational Modeling in Pharmaceutical Development. *J. Chem. Inf. Model.* **2022**, 62 (5), 1160–1171.
- (28) Chow, K.; Tong, H. H. Y.; Lum, S.; Chow, A. H. L. Engineering of pharmaceutical materials: An industrial perspective. *J. Pharm. Sci.* **2008**, *97* (8), 2855–2877.
- (29) Rantanen, J.; Khinast, J. The Future of Pharmaceutical Manufacturing Sciences. J. Pharm. Sci. 2015, 104 (11), 3612–3638.
- (30) Cote, A.; Erdemir, D.; Girard, K. P.; Green, D. A.; Lovette, M. A.; Sirota, E.; Nere, N. K. Perspectives on the Current State, Challenges, and Opportunities in Pharmaceutical Crystallization Process Development. *Cryst. Growth Des.* **2020**, 20 (12), 7568–7581.
- (31) Reilly, A. M.; Cooper, R. I.; Adjiman, C. S.; Bhattacharya, S.; Boese, A. D.; Brandenburg, J. G.; Bygrave, P. J.; Bylsma, R.; Campbell, J. E.; Car, R.; et al. Report on the sixth blind test of organic crystal structure prediction methods. *Acta Crystallogr. B* **2016**, 72 (4), 439–459.
- (32) Llinas, A.; Oprisiu, I.; Avdeef, A. Findings of the Second Challenge to Predict Aqueous Solubility. *J. Chem. Inf. Model.* **2020**, *60* (10), 4791–4803.
- (33) Price, S. L. Progress in understanding crystallisation: A personal perspective. *Faraday Discuss.* **2022**, 235, 569–581.
- (34) Lovette, M. A.; Albrecht, J.; Ananthula, R. S.; Ricci, F.; Sangodkar, R.; Shah, M. S.; Tomasi, S. Evaluation of Predictive Solubility Models in Pharmaceutical Process Development—an Enabling Technologies Consortium Collaboration. *Cryst. Growth Des.* **2022**, 22 (9), 5239–5263.
- (35) Reutzel-Edens, S. M.; Bhardwaj, R. M. Crystal forms in pharmaceutical applications: olanzapine, a gift to crystal chemistry that keeps on giving. *IUCrJ* **2020**, *7*, 955–964.
- (36) Boye, K.; Ross, M.; Mody, R.; Konig, M.; Gelhorn, H. Patients' preferences for once-daily oral versus once-weekly injectable diabetes medications: The REVISE study. *Diabetes Obes. Metab.* **2021**, 23 (2), 508–519.
- (37) Abramov, Y. A. Rational Solvent Selection for Pharmaceutical Impurity Purge. Cryst. Growth Des. 2018, 18 (2), 1208–1214.
- (38) Abramov, Y. A.; Zelellow, A.; Chen, C.; Wang, J.; Sekharan, S. Novel Computational Approach to Guide Impurities Rejection by Crystallization: A Case Study of MRTX849 Impurities. *Cryst. Growth Des.* **2022**, 22 (12), 6844–6848.
- (39) Burcham, C. L.; Florence, A. J.; Johnson, M. D. Continuous Manufacturing in Pharmaceutical Process Development and Manufacturing. *Annu. Rev. Chem. Biomol.* **2018**, 9 (1), 253–281.

- (40) Bauer, J.; Spanton, S.; Henry, R.; Quick, J.; Dziki, W.; Porter, W.; Morris, J. Ritonavir: An extraordinary example of conformational polymorphism. *Pharm. Res.* **2001**, *18* (6), 859–866.
- (41) Bucar, D. K.; Lancaster, R. W.; Bernstein, J. Disappearing Polymorphs Revisited. *Angew. Chem., Int. Ed.* **2015**, *54* (24), 6972–6993.
- (42) Chemburkar, S. R.; Bauer, J.; Deming, K.; Spiwek, H.; Patel, K.; Morris, J.; Henry, R.; Spanton, S.; Dziki, W.; Porter, W.; et al. Dealing with the impact of ritonavir polymorphs on the late stages of bulk drug process development. *Org. Process Res. Dev.* **2000**, *4* (5), 413–417.
- (43) Morissette, S. L.; Soukasene, S.; Levinson, D.; Cima, M. J.; Almarsson, O. Eludication of crystal form diversity of the HIV protease inhibitor ritonavir by high-throughput crystallisation. *P. Natl. Acad. Sci. U.S.A.* **2003**, *100* (5), 2180–2184.
- (44) Yamaguchi, S.; Kaneko, M.; Narukawa, M. Approval success rates of drug candidates based on target, action, modality, application, and their combinations. *CTS-Clin. Transl. Sci.* **2021**, *14* (3), 1113–1122.
- (45) Braga, D.; Casali, L.; Grepioni, F. The Relevance of Crystal Forms in the Pharmaceutical Field: Sword of Damocles or Innovation Tools? *Int. J. Mol. Sci.* **2022**, 23 (16), 9013.
- (46) Newman, A. Specialized Solid Form Screening Techniques. Org. Process Res. Dev. 2013, 17 (3), 457–471.
- (47) Price, S. L.; Reutzel-Edens, S. M. The potential of computed crystal energy landscapes to aid solid-form development. *Drug Discover. Today* **2016**, *21* (6), 912–923.
- (48) Bernstein, J. Polymorphism in Molecular Crystals; Clarendon Press, 2020.
- (49) Reutzel-Edens, S. M.; Braun, D. E.; Newman, A. W. Hygroscopicity and Hydrates in Pharmaceutical Solids. *Polymorphism Pharm. Ind.* **2018**, 159–188.
- (50) Price, S. L. Is zeroth order crystal structure prediction (CSP\_0) coming to maturity? What should we aim for in an ideal crystal structure prediction code? *Faraday Discuss.* **2018**, *211*, 9–30.
- (51) Belenguer, A. M.; Lampronti, G. I.; Cruz-Cabeza, A. J.; Hunter, C. A.; Sanders, J. K. M. Solvation and surface effects on polymorph stabilities at the nanoscale. *Chem. Sci.* **2016**, *7* (11), 6617–6627.
- (52) Ward, M. D. Perils of Polymorphism: Size Matters. *Israel J. Chem.* **2017**, 57 (1–2), 82–92.
- (53) Firaha, D.; Liu, Y. M.; van de Streek, J.; Sasikumar, K.; Dietrich, H.; Helfferich, J.; Aerts, L.; Braun, D. E.; Broo, A.; DiPasquale, A. G.; et al. Predicting crystal form stability under real-world conditions. *Nature* **2023**, 623 (7986), 324–328.
- (54) Braun, D. E.; McMahon, J. A.; Bhardwaj, R. M.; Nyman, J.; Neumann, M. A.; van de Streek, J.; Reutzel-Edens, S. M. Inconvenient Truths about Solid Form Landscapes Revealed in the Polymorphs and Hydrates of Gandotinib. *Cryst. Growth Des.* **2019**, *19* (5), 2947–2962.
- (55) Price, S. L. Why don't we find more polymorphs? *Acta Crystallogr. B* **2013**, *69*, 313–328.
- (56) Bryenton, K. R.; Adeleke, A. A.; Dale, S. G.; Johnson, E. R. Delocalization error: The greatest outstanding challenge in density-functional theory. *Wiley Interdiscip. Rev.: Comput. Mol. Sci.* **2023**, 13 (2), No. e1631.
- (57) Francia, N. F.; Price, L. S.; Nyman, J.; Price, S. L.; Salvalaglio, M. Systematic Finite-Temperature Reduction of Crystal Energy Landscapes. *Cryst. Growth Des.* **2020**, *20*, 6847–6862.
- (58) Lucaioli, P.; Nauha, E.; Gimondi, I.; Price, L. S.; Guo, R.; Iuzzolino, L.; Singh, I.; Salvalaglio, M.; Price, S. L.; Blagden, N. Serendipitous isolation of a disappearing conformational polymorph of succinic acid challenges computational polymorph prediction. *CrystEngComm* **2018**, 20 (28), 3971–3977.
- (59) Bhardwaj, R. M.; Price, L. S.; Price, S. L.; Reutzel-Edens, S. M.; Miller, G. J.; Oswald, I. D. H.; Johnston, B.; Florence, A. J. Exploring the Experimental and Computed Crystal Energy Landscape of Olanzapine. *Cryst. Growth Des.* **2013**, *13* (4), 1602–1617.
- (60) Askin, S.; Cockcroft, J. K.; Price, L. S.; Goncalves, A. D.; Zhao, M.; Tocher, D. A.; Williams, G. R.; Gaisford, S.; Craig, D. Q. M. Olanzapine Form IV: Discovery of a New Polymorphic Form Enabled

- by Computed Crystal Energy Landscapes. Cryst. Growth Des. 2019, 19 (5), 2751–2757.
- (61) LeBlanc, L. M.; Johnson, E. R. Crystal-energy landscapes of active pharmaceutical ingredients using composite approaches. *CrystEngComm* **2019**, 21 (40), 5995–6009.
- (62) Warzecha, M.; Guo, R.; Bhardwaj, R. M.; Reutzel-Edens, S. M.; Price, S. L.; Lamprou, D. A.; Florence, A. J. Direct Observation of Templated Two-Step Nucleation Mechanism during Olanzapine Hydrate Formation. *Cryst. Growth Des.* **2017**, *17* (12), 6382–6393.
- (63) Warzecha, M.; Safari, M. S.; Florence, A. J.; Vekilov, P. G. Mesoscopic Solute-Rich Clusters in Olanzapine Solutions. *Cryst. Growth Des.* **2017**, *17* (12), 6668–6676.
- (64) Warzecha, M.; Verma, L.; Johnston, B. F.; Palmer, J. C.; Florence, A. J.; Vekilov, P. G. Olanzapine crystal symmetry originates in preformed centrosymmetric solute dimers. *Nat. Chem.* **2020**, *12* (10), 914–920.
- (65) Francia, N. F.; Price, L. S.; Salvalaglio, M. Reducing crystal structure overprediction of ibuprofen with large scale molecular dynamics simulations. *CrystEngComm* **2021**, 23 (33), 5575–5584.
- (66) van Eijck, B. P.; Kroon-Batenburg, L. M. J.; Kroon, J. Energy minimisation and Molecular Dynamics calculations for molecular crystals. In *Theoretical Aspects and Computer Modeling of the Molecular Solid State*, Gavezzotti, A., Ed.; John Wiley & Sons, 1997; pp. 99146.
- (67) Gavezzotti, A. A molecular dynamics test of the different stability of crystal polymorphs under thermal strain. *J. Am. Chem. Soc.* **2000**, *122* (43), 10724–10725.
- (68) Yang, S.; Day, G. M. Global analysis of the energy landscapes of molecular crystal structures by applying the threshold algorithm. *Commun. Chem.* **2022**, *5* (1), 86.
- (69) Nyman, J.; Day, G. M. Modelling temperature-dependent properties of polymorphic organic molecular crystals. *Phys. Chem. Chem. Phys.* **2016**, *18* (45), 31132–31143.
- (70) Buchholz, H. K.; Hylton, R. K.; Brandenburg, J. G.; Seidel-Morgenstern, A.; Lorenz, H.; Stein, M.; Price, S. L. Thermochemistry of Racemic and Enantiopure Organic Crystals for Predicting Enantiomer Separation. *Cryst. Growth Des.* **2017**, *17* (9), 4676–4686.
- (71) Reilly, A. M.; Tkatchenko, A. Role of Dispersion Interactions in the Polymorphism and Entropic Stabilization of the Aspirin Crystal. *Phys. Rev. Lett.* **2014**, *113* (5), 055701.
- (72) Hill, T. L. An Introduction to Statistical Tharmodynamics; Addison-Wesley Publishing Company, Inc.; Courier Corporation, 1960; p 1986.
- (73) Tuckerman, M. E. Statistical Mechanics: Theory and Molecular Simulation; Oxford University Press, 2010.
- (74) Frenkel, D.; Smit, B. Understanding molecular simulation: From algorithms to applications; Elsevier, 2001.
- (75) Frenkel, D.; Ladd, A. J. C. New Monte Carlo method to compute the free energy of arbitrary solids. Application to the fcc and hcp phases of hard spheres. *J. Chem. Phys.* **1984**, *81* (7), 3188–3193.
- (76) Vega, C.; Noya, E. G. Revisiting the Frenkel-Ladd method to compute the free energy of solids: The Einstein molecule approach. *J. Chem. Phys.* **2007**, *127* (15), 154113.
- (77) Sweatman, M. B.; Atamas, A. A.; Leyssale, J.-M. The self-referential method combined with thermodynamic integration. *J. Chem. Phys.* **2008**, 128 (6), 064102.
- (78) Monson, P. A.; Kofke, D. A. Solid-Fluid Equilibrium: Insights from Simple Molecular Models. *Adv. Chem. Phys.* **2000**, *115*, 113–179.
- (79) Li, L.; Totton, T.; Frenkel, D. Computational methodology for solubility prediction: Application to the sparingly soluble solutes. *J. Chem. Phys.* **2017**, *146* (21), 214110.
- (80) Aragones, J. L.; Valeriani, C.; Vega, C. Note: Free energy calculations for atomic solids through the Einstein crystal/molecule methodology using GROMACS and LAMMPS. *J. Chem. Phys.* **2012**, 137 (14), 146101.
- (81) Aragones, J. L.; Noya, E. G.; Valeriani, C.; Vega, C. Free energy calculations for molecular solids using GROMACS. *J. Chem. Phys.* **2013**, *139* (3), 034104.

- (82) Reddy A, R. K.; Punnathanam, S. N. Calculation of excess free energy of molecular solids comprised of flexible molecules using Einstein molecule method. *Mol. Simul.* **2018**, *44* (10), 781–788.
- (83) Bruce, A. D.; Wilding, N. B.; Ackland, G. J. Free Energy of Crystalline Solids: A Lattice-Switch Monte Carlo Method. *Phys. Rev. Lett.* **1997**, *79* (16), 3002–3005.
- (84) Bruce, A. D.; Jackson, A. N.; Ackland, G. J.; Wilding, N. B. Lattice-switch Monte Carlo method. *Phys. Rev. E* **2000**, *61* (1), 906–919.
- (85) Wilms, D.; Wilding, N. B.; Binder, K. Transitions between imperfectly ordered crystalline structures: A phase switch Monte Carlo study. *Phys. Rev. E* **2012**, *85* (5), 056703.
- (86) Zwanzig, R. W. High-Temperature Equation of State by a Perturbation Method. I. Nonpolar Gases. *J. Chem. Phys.* **1954**, 22 (8), 1420–1426.
- (87) Bennett, C. H. Efficient estimation of free energy differences from Monte Carlo data. *J. Comput. Phys.* **1976**, 22 (2), 245–268.
- (88) Kamat, K.; Peters, B. Diabat Interpolation for Polymorph Free-Energy Differences. J. Phys. Chem. Lett. 2017, 8 (3), 655–660.
- (89) Kamat, K.; Peters, B. Gibbs free-energy differences between polymorphs via a diabat approach. *J. Chem. Phys.* **2018**, *149* (21), 214106.
- (90) Kamat, K.; Guo, R.; Reutzel-Edens, S. M.; Price, S. L.; Peters, B. Diabat method for polymorph free energies: Extension to molecular crystals. *J. Chem. Phys.* **2020**, *1*53 (24), 244105.
- (91) Torrie, G. M.; Valleau, J. P. Nonphysical sampling distributions in Monte Carlo free-energy estimation: Umbrella sampling. *J. Comput. Phys.* **1977**, 23 (2), 187–199.
- (92) Roux, B. The calculation of the potential of mean force using computer simulations. *Comput. Phys. Commun.* **1995**, *91* (1), 275–282.
- (93) Laio, A.; Parrinello, M. Escaping free-energy minima. *P. Natl. Acad. Sci. U.S.A.* **2002**, 99 (20), 12562–12566.
- (94) Barducci, A.; Bussi, G.; Parrinello, M. Well-tempered metadynamics: A smoothly converging and tunable free-energy method. *Phys. Rev. Lett.* **2008**, *100* (2), 020603.
- (95) Barducci, A.; Bonomi, M.; Parrinello, M. Metadynamics. *Wiley Interdiscip. Rev.: Comput. Mol. Sci.* **2011**, *1* (5), 826–843.
- (96) Kästner, J. Umbrella sampling. Wiley Interdiscip. Rev.: Comput. Mol. Sci. 2011, 1 (6), 932–942.
- (97) Kästner, J.; Thiel, W. Bridging the gap between thermodynamic integration and umbrella sampling provides a novel analysis method: "Umbrella integration. *J. Chem. Phys.* **2005**, *123* (14), 144104.
- (98) Marinova, V.; Salvalaglio, M. Time-independent free energies from metadynamics via mean force integration. *J. Chem. Phys.* **2019**, 151 (16), 164115.
- (99) Giberti, F.; Cheng, B.; Tribello, G. A.; Ceriotti, M. Iterative Unbiasing of Quasi-Equilibrium Sampling. *J. Chem. Theory Comput.* **2020**, *16* (1), 100–107.
- (100) Tiwary, P.; Parrinello, M. A Time-Independent Free Energy Estimator for Metadynamics. *J. Phys. Chem. B* **2015**, *119* (3), 736–742.
- (101) Bonomi, M.; Barducci, A.; Parrinello, M. Reconstructing the equilibrium Boltzmann distribution from well-tempered metadynamics. *J. Comput. Chem.* **2009**, *30* (11), 1615–1621.
- (102) Cuendet, M. A.; Tuckerman, M. E. Free Energy Reconstruction from Metadynamics or Adiabatic Free Energy Dynamics Simulations. *J. Chem. Theory Comput.* **2014**, *10* (8), 2975–2986.
- (103) Rosso, L.; Tuckerman, M. E. An Adiabatic Molecular Dynamics Method for the Calculation of Free Energy Profiles. *Mol. Simul.* **2002**, 28 (1–2), 91–112.
- (104) Schneider, E.; Vogt, L.; Tuckerman, M. E. Exploring polymorphism of benzene and naphthalene with free energy based enhanced molecular dynamics. *Acta Crystallogr. B* **2016**, 72, 542–550.
- (105) Abrams, J. B.; Tuckerman, M. E. Efficient and Direct Generation of Multidimensional Free Energy Surfaces via Adiabatic Dynamics without Coordinate Transformations. *J. Phys. Chem. B* **2008**, *112* (49), 15742–15757.

- (106) Yu, T.-Q.; Tuckerman, M. E. Temperature-Accelerated Method for Exploring Polymorphism in Molecular Crystals Based on Free Energy. *Phys. Rev. Lett.* **2011**, *107* (1), 015701.
- (107) Yu, T.-Q.; Chen, P.-Y.; Chen, M.; Samanta, A.; Vanden-Eijnden, E.; Tuckerman, M. Order-parameter-aided temperature-accelerated sampling for the exploration of crystal polymorphism and solid-liquid phase transitions. *J. Chem. Phys.* **2014**, *140* (21), 214109. (108) Kapil, V.; Engel, E. A. A complete description of thermodynamic stabilities of molecular crystals. *P. Natl. Acad. Sci. U.S.A.* **2022**, *119* (6), No. e2111769119.
- (109) Luo, H. Y.; Hao, X.; Gong, Y. Q.; Zhou, J. H.; He, X.; Li, J. Rational Crystal Polymorph Design of Olanzapine. *Cryst. Growth Des.* **2019**, *19* (4), 2388–2395.
- (110) Tang, J. Q.; Han, Y. Q.; Ali, I.; Luo, H. Y.; Nowak, A.; Li, J. J. Stability and phase transition investigation of olanzapine polymorphs. *Chem. Phys. Lett.* **2021**, *767*, 138384.
- (111) Sosso, G. C.; Chen, J.; Cox, S. J.; Fitzner, M.; Pedevilla, P.; Zen, A.; Michaelides, A. Crystal Nucleation in Liquids: Open Questions and Future Challenges in Molecular Dynamics Simulations. *Chem. Rev.* **2016**, *116* (12), 7078–7116.
- (112) Brittain, H. G. Polymorphism in Pharmaceutical Solids, Brittain, H. G. Eds; Informa Healthcare, 2016.
- (113) Neumann, M. A.; van de Streek, J. How many ritonavir cases are there still out there? *Faraday Discuss.* **2018**, *211*, 441–458.
- (114) Neumann, M. A.; van de Streek, J.; Fabbiani, F. P. A.; Hidber, P.; Grassmann, O. Combined crystal structure prediction and high-pressure crystallization in rational pharmaceutical polymorph screening. *Nat. Commun.* **2015**, *6*, 7793.
- (115) Oswald, I. D. H.; Chataigner, I.; Elphick, S.; Fabbiani, F. P. A.; Lennie, A. R.; Maddaluno, J.; Marshall, W. G.; Prior, T. J.; Pulham, C. R.; Smith, R. I. Putting pressure on elusive polymorphs and solvates. *CrystEngComm* **2009**, *11* (2), 359–366.
- (116) Potticary, J.; Hall, C. L.; Guo, R.; Price, S. L.; Hall, S. R. On the Application of Strong Magnetic Fields during Organic Crystal Growth. *Cryst. Growth Des.* **2021**, *21* (11), 6254–6265.
- (117) Day, G. M.; Cooper, A. I. Energy-Structure-Function Maps: Cartography for Materials Discovery. *Adv. Mater.* **2018**, *30* (37), 1704944.
- (118) Greenaway, R. L.; Jelfs, K. E. Integrating Computational and Experimental Workflows for Accelerated Organic Materials Discovery. *Adv. Mater.* **2021**, 33 (11), 2004831.
- (119) McArdle, P.; Erxleben, A. Sublimation a green route to new solid-state forms. *CrystEngComm* **2021**, *23*, 5965–5975.
- (120) Srirambhatla, V. K.; Guo, R.; Price, S. L.; Florence, A. J. Isomorphous template induced crystallisation: a robust method for the targeted crystallisation of computationally predicted metastable polymorphs. *Chem. Commun.* **2016**, *52*, 7384–7386.
- (121) Case, D. H.; Srirambhatla, V. K.; Guo, R.; Watson, R. E.; Price, L. S.; Polyzois, H.; Cockcroft, J. K.; Florence, A. J.; Tocher, D. A.; Price, S. L. Successful Computationally Directed Templating of Metastable Pharmaceutical Polymorphs. *Cryst. Growth Des.* **2018**, *18* (9), 5322–5331.
- (122) Brandenburg, J. G.; Potticary, J.; Sparkes, H. A.; Price, S. L.; Hall, S. R. Thermal Expansion of Carbamazepine: Systematic Crystallographic Measurements Challenge Quantum Chemical Calculations. J. Phys. Chem. Lett. 2017, 8 (17), 4319–4324.
- (123) McKinley, J. L.; Beran, G. J. O. Identifying pragmatic quasiharmonic electronic structure approaches for modeling molecular crystal thermal expansion. *Faraday Discuss.* **2018**, *211*, 181–207.
- (124) Souvatzis, P.; Eriksson, O.; Katsnelson, M. I.; Rudin, S. P. Entropy Driven Stabilization of Energetically Unstable Crystal Structures Explained from First Principles Theory. *Phys. Rev. Lett.* **2008**, *100* (9), 095901.
- (125) Hellman, O.; Abrikosov, I. A.; Simak, S. I. Lattice dynamics of anharmonic solids from first principles. *Phys. Rev. B* **2011**, *84* (18), 180301.
- (126) Giberti, F.; Salvalaglio, M.; Mazzotti, M.; Parrinello, M. Insight into the nucleation of urea crystals from the melt. *Chem. Eng. Sci.* **2015**, *121*, 51–59.

- (127) Giberti, F.; Salvalaglio, M.; Parrinello, M. Metadynamics studies of crystal nucleation. *IUCrJ* **2015**, 2 (2), 256–266.
- (128) Gimondi, I.; Salvalaglio, M. CO2 packing polymorphism under pressure: Mechanism and thermodynamics of the I-III polymorphic transition. *J. Chem. Phys.* **2017**, *147* (11), 114502.
- (129) Piaggi, P. M.; Parrinello, M. Predicting polymorphism in molecular crystals using orientational entropy. *P. Natl. Acad. Sci. U.S.A.* **2018**, *115* (41), 10251–10256.
- (130) Piaggi, P. M.; Valsson, O.; Parrinello, M. Enhancing Entropy and Enthalpy Fluctuations to Drive Crystallization in Atomistic Simulations. *Phys. Rev. Lett.* **2017**, *119* (1), 015701.
- (131) Song, H. X.; Vogt-Maranto, L.; Wiscons, R.; Matzger, A. J.; Tuckerman, M. E. Generating Cocrystal Polymorphs with Information Entropy Driven by Molecular Dynamics-Based Enhanced Sampling. J. Phys. Chem. Lett. 2020, 11 (22), 9751–9758.
- (132) Metz, M. P.; Shahbaz, M.; Song, H. X.; Vogt-Maranto, L.; Tuckerman, M. E.; Szalewicz, K. Crystal Structure Predictions for 4-Amino-2,3,6-trinitrophenol Using a Tailor-Made First-Principles-Based Force Field. *Cryst. Growth Des.* **2022**, 22 (2), 1182–1195.
- (133) Gobbo, G.; Bellucci, M. A.; Tribello, G. A.; Ciccotti, G.; Trout, B. L. Nucleation of Molecular Crystals Driven by Relative Information Entropy. *J. Chem. Theory Comput.* **2018**, *14* (2), 959–972
- (134) Cardew, P. T.; Davey, R. J. The kinetics of solvent-mediated phase transformations. P. R. Soc. London A Mater. 1985, 398 (1815), 415–428.
- (135) De Yoreo, J. J.; Zepeda-Ruiz, L. A.; Friddle, R. W.; Qiu, S. R.; Wasylenki, L. E.; Chernov, A. A.; Gilmer, G. H.; Dove, P. M. Rethinking Classical Crystal Growth Models through Molecular Scale Insights: Consequences of Kink-Limited Kinetics. *Cryst. Growth Des.* **2009**, *9* (12), 5135–5144.
- (136) Li, J. J.; Tilbury, C. J.; Joswiak, M. N.; Peters, B.; Doherty, M. F. Rate Expressions for Kink Attachment and Detachment During Crystal Growth. *Cryst. Growth Des.* **2016**, *16* (6), 3313–3322.
- (137) Stack, A. G. Molecular Dynamics Simulations of Solvation and Kink Site Formation at the {001} Barite–Water Interface. *J. Phys. Chem. C* 2009, 113 (6), 2104–2110.
- (138) Joswiak, M. N.; Doherty, M. F.; Peters, B. Critical length of a one-dimensional nucleus. *J. Chem. Phys.* **2016**, *145* (21), 211916.
- (139) De La Pierre, M.; Raiteri, P.; Stack, A. G.; Gale, J. D. Uncovering the Atomistic Mechanism for Calcite Step Growth. *Angew. Chem., Int. Ed.* **2017**, *56* (29), 8464–8467.
- (140) Benavides, A. L.; Aragones, J. L.; Vega, C. Consensus on the solubility of NaCl in water from computer simulations using the chemical potential route. *J. Chem. Phys.* **2016**, *144* (12), 124504.
- (141) Salvalaglio, M.; Perego, C.; Giberti, F.; Mazzotti, M.; Parrinello, M. Molecular-dynamics simulations of urea nucleation from aqueous solution. *P. Natl. Acad. Sci. U.S.A.* **2015**, *112* (1), E6–E14.
- (142) Kolafa, J. Solubility of NaCl in water and its melting point by molecular dynamics in the slab geometry and a new BK3-compatible force field. *J. Chem. Phys.* **2016**, *145* (20), 204509.
- (143) Nielsen, A. E. Kinetics of Precipitation; Pergamon Press, 1964. (144) Weeks, J. D.; Gilmer, G. H. Dynamics of Crystal Growth. Adv. Chem. Phys. 1979, 40, 157–228.
- (145) Chernov, A. A. Present-day understanding of crystal growth from aqueous solutions. *Prog. Cryst. Growth Charact. Mater.* **1993**, 26, 121–151.
- (146) Joswiak, M. N.; Doherty, M. F.; Peters, B. Ion dissolution mechanism and kinetics at kink sites on NaCl surfaces. *P. Natl. Acad. Sci. U.S.A* **2018**, *115* (4), 656–661.
- (147) Bjelobrk, Z.; Mendels, D.; Karmakar, T.; Parrinello, M.; Mazzotti, M. Solubility Prediction of Organic Molecules with Molecular Dynamics Simulations. *Cryst. Growth Des.* **2021**, *21* (9), 5198–5205.
- (148) Bjelobrk, Z.; Rajagopalan, A. K.; Mendels, D.; Karmakar, T.; Parrinello, M.; Mazzotti, M. Solubility of Organic Salts in Solvent—Antisolvent Mixtures: A Combined Experimental and Molecular

- Dynamics Simulations Approach. J. Chem. Theory Comput. 2022, 18 (8), 4952-4959.
- (149) Khanna, V.; Doherty, M. F.; Peters, B. Absolute chemical potentials for complex molecules in fluid phases: A centroid reference for predicting phase equilibria. *J. Chem. Phys.* **2020**, 153 (21), 214504.
- (150) Khanna, V.; Doherty, M. F.; Peters, B. Predicting solubility and driving forces for crystallization using the absolute chemical potential route. *Mol. Phys.* **2023**, *121* (2), No. e2155595.
- (151) Berendsen, H. J. C.; Grigera, J. R.; Straatsma, T. P. The Missing Term in Effective Pair Potentials. J. Phys. Chem. 1987, 91 (24), 6269–6271.
- (152) Widom, B. Some Topics in the Theory of Fluids. J. Chem. Phys. 1963, 39 (11), 2808-2812.
- (153) Siepmann, J. I.; Frenkel, D. Configurational bias Monte Carlo: a new sampling scheme for flexible chains. *Mol. Phys.* **1992**, *75* (1), 59–70.
- (154) Shi, W.; Maginn, E. J. Continuous Fractional Component Monte Carlo: An Adaptive Biasing Method for Open System Atomistic Simulations. *J. Chem. Theory Comput.* **2007**, 3 (4), 1451–1463.
- (155) Weeks, J. D.; Chandler, D.; Andersen, H. C. Role of Repulsive Forces in Determining the Equilibrium Structure of Simple Liquids. *J. Chem. Phys.* **1971**, *54* (12), 5237–5247.
- (156) Shivakumar, D.; Williams, J.; Wu, Y.; Damm, W.; Shelley, J.; Sherman, W. Prediction of Absolute Solvation Free Energies using Molecular Dynamics Free Energy Perturbation and the OPLS Force Field. *J. Chem. Theory Comput.* **2010**, *6* (5), 1509–1519.
- (157) Mobley, D. L.; Guthrie, J. P. FreeSolv: a database of experimental and calculated hydration free energies, with input files. *J. Comput. Aid. Mol. Des.* **2014**, 28 (7), 711–720.
- (158) Khanna, V.; Monroe, J. I.; Doherty, M. F.; Peters, B. Performing solvation free energy calculations in LAMMPS using the decoupling approach. *J. Comput. Aid. Mol. Des.* **2020**, 34 (6), 641–646
- (159) Yu, Q.; Black, S.; Wei, H. Solubility of Butanedioic Acid in Different Solvents at Temperatures between 283 K and 333 K. *J. Chem. Eng. Data.* **2009**, 54 (7), 2123–2125.
- (160) Fowles, D. J.; Palmer, D. S.; Guo, R.; Price, S. L.; Mitchell, J. B. O. Toward Physics-Based Solubility Computation for Pharmaceuticals to Rival Informatics. *J. Chem. Theory Comput.* **2021**, *17* (6), 3700–3709.
- (161) Rees, D. C.; Wolfe, G. M. Macromolecular solvation energies derived from small-molecule crystal morphology. *Protein Sci.* **1993**, 2 (11), 1882–1889.
- (162) da Silva, M. A. V.; Monte, M. J. S.; Ribeiro, J. R. Thermodynamic study on the sublimation of succinic acid and of methyl- and dimethyl-substituted succinic and glutaric acids. *J. Chem. Thermodyn.* **2001**, 33 (1), 23–31.
- (163) Homeyer, N.; Gohlke, H. Free Energy Calculations by the Molecular Mechanics Poisson—Boltzmann Surface Area Method. *Mol. Inform.* **2012**, *31* (2), 114–122.
- (164) Cossi, M.; Barone, V.; Cammi, R.; Tomasi, J. Ab initio study of solvated molecules: A new implementation of the polarizable continuum model. *Chem. Phys. Lett.* **1996**, 255 (4), 327–335.
- (165) Mullins, E.; Oldland, R.; Liu, Y. A.; Wang, S.; Sandler, S. I.; Chen, C.-C.; Zwolak, M.; Seavey, K. C. Sigma-Profile Database for Using COSMO-Based Thermodynamic Methods. *Ind. Eng. Chem. Res.* **2006**, *45* (12), 4389–4415.
- (166) Abramov, Y. A.; Sun, G. X.; Zeng, Q.; Yang, M. J. Guiding Lead Optimization for Solubility Improvement with Physics-Based Modeling. *Mol. Pharmaceut.* **2020**, *17* (2), 666–673.
- (167) Median (50th percentile) particle diameter for a volumetric particle size distribution assuming spherical particles. More generally Xv50 where X is a characteristic length for a volumetric particle size distribution.
- (168) Shayesteh Zadeh, A.; Peters, B. Conformational Interconversion Kinetics, Boundary Layer Transport, and Crystal Growth Impedance. *Cryst. Growth Des.* **2022**, 22 (7), 4298–4304.

(169) Vekilov, P. G. Nucleation. Cryst. Growth Des. 2010, 10 (12), 5007-5019.

Article

- (170) Burton, W. K.; Cabrera, N.; Frank, F. C. The growth of crystals and the equilibrium structure of their surfaces. *Philos. T. R. Soc. A* **1951**, 243 (866), 299–358.
- (171) Ohara, M.; Reid, R. C. Modelling Crystal Growth Rates from Solution; Prentice-Hall, 1973.
- (172) Lovette, M. A.; Browning, A. R.; Griffin, D. W.; Sizemore, J. P.; Snyder, R. C.; Doherty, M. F. Supporting Information in: Crystal Shape Engineering. *Ind. Eng. Chem. Res.* **2008**, 47 (24), 9812–9833. (173) Chernov, A. A. The Spiral Growth Of Crystals. *Sov. Phys. Uspekhi* **1961**, 4 (1), 116–148.
- (174) Chernov, A. A. Modern Crystallography III, Crystal Growth; Springer-Verlag, 1984.
- (175) Lovette, M. A.; Doherty, M. F. Reinterpreting edge energies calculated from crystal growth experiments. *J. Cryst. Growth* **2011**, 327 (1), 117–126.
- (176) Tilbury, C. J.; Doherty, M. F. Modeling layered crystal growth at increasing supersaturation by connecting growth regimes. *AIChE J.* **2017**, *63* (4), 1338–1352.
- (177) Teng, H. H.; Dove, P. M.; Orme, C. A.; De Yoreo, J. J. Thermodynamics of Calcite Growth: Baseline for Understanding Biomineral Formation. *Science* **1998**, 282 (5389), 724–727.
- (178) Voronkov, V. V. Dislocation mechanism of growth with a low kink density. Sov. Phys. Crystallogr. 1973, 18 (1), 19–23.
- (179) Israelachvili, J. N. Chapter 17. In *Intermolecular and Surface Forces*; Academic Press, 2011.
- (180) Winn, D.; Doherty, M. F. A new technique for predicting the shape of solution-grown organic crystals. *AIChE J.* **1998**, *44* (11), 2501–2514.
- (181) Winn, D.; Doherty, M. F. Predicting the shape of organic crystals grown from polar solvents. *Chem. Eng. Sci.* **2002**, *57* (10), 1805–1813.
- (182) Tilbury, C. J.; Green, D. A.; Marshall, W. J.; Doherty, M. F. Predicting the Effect of Solvent on the Crystal Habit of Small Organic Molecules. *Cryst. Growth Des.* **2016**, *16* (5), 2590–2604.
- (183) Sours, R. E.; Zellelow, A. Z.; Swift, J. A. An in Situ Atomic Force Microscopy Study of Uric Acid Crystal Growth. *J. Phys. Chem. B* **2005**, *109* (20), 9989–9995.
- (184) Vekilov, P. G. What Determines the Rate of Growth of Crystals from Solution? *Cryst. Growth Des.* **2007**, 7 (12), 2796–2810.
- (185) Rimer, J. D.; An, Z.; Zhu, Z.; Lee, M. H.; Goldfarb, D. S.; Wesson, J. A.; Ward, M. D. Crystal Growth Inhibitors for the Prevention of l-Cystine Kidney Stones Through Molecular Design. *Science* **2010**, 330 (6002), 337–341.
- (186) Hartman, P.; Perdok, W. G. On the Relations Between Structure and Morphology of Crystals. I. *Acta Crystallogr.* **1955**, 8 (1), 49–52.
- (187) Hartman, P.; Perdok, W. G. On the Relations Between Structure and Morphology of Crystals. II. *Acta Crystallogr.* **1955**, 8 (9), 521–524.
- (188) Hartman, P.; Perdok, W. G. On the Relations Between Structure and Morphology of Crystals. III. *Acta Crystallogr.* **1955**, 8 (9), 525–529.
- (189) Gibbs, J. W. The Scientific Papers of J. In Willard Gibbs: vol. One Thermodynamics; Dover Publications, 1961.
- (190) Frank, F. C. On the kinematic theory of crystal growth and dissolution processes. In *Growth and Perfection of Crystals*, Doremus, R. H.; Roberts, B. W.; Turnbull, D., Ed.; John Wiley and Sons, 1958; pp. 411419.
- (191) Chernov, A. A. The kinetics of the growth forms of crystals. Sov. Phys. Crystallogr. 1963, 7, 728–730.
- (192) Lovette, M. A.; Doherty, M. F. Predictive Modeling of Supersaturation-Dependent Crystal Shapes. *Cryst. Growth Des.* **2012**, 12 (2), 656–669.
- (193) Li, J.; Tilbury, C. J.; Kim, S. H.; Doherty, M. F. A design aid for crystal growth engineering. *Prog. Mater. Sci.* **2016**, *82*, 1–38.
- (194) Gavezzotti, A. Efficient computer modeling of organic materials. The atom-atom, Coulomb-London-Pauli (AA-CLP)

- model for intermolecular electrostatic-polarization, dispersion and repulsion energies. New J. Chem. 2011, 35 (7), 1360–1368.
- (195) Van Oss, C. J.; Chaudhury, M. K.; Good, R. J. Interfacial Lifshitz-van der Waals and polar interactions in macroscopic systems. *Chem. Rev.* **1988**, 88 (6), 927–941.
- (196) Wawrzycka-Gorczyca, I.; Koziol, A. E.; Glice, M.; Cybulski, J. Polymorphic form II of 2-methyl-4-(4-methyl-1-piperazinyl)-10H-thieno[2,3-b][1,5]benzodiazepine. *Acta Crystallogr. E* **2004**, *60*, o66–o68.
- (197) Wawrzycka-Gorczyca, I.; Mazur, L.; Koziol, A. E. 2-methyl-4-(4-methyl-1-piperazinyl)-10H-thieno[2,3-b][1,5]benzodiazepine methanol solvate. *Acta Crystallogr. E* **2004**, *60*, *69*–*67*1.
- (198) Wawrzycka-Gorczyca, I.; Borowski, P.; Osypiuk-Tomasik, J.; Mazur, L.; Koziol, A. E. Crystal structure of olanzapine and its solvates. Part 3. Two and three-component solvates with water, ethanol, butan-2-ol and dichloromethane. *J. Mol. Struct.* **2007**, 830 (1–3), 188–197.
- (199) Verma, L.; Warzecha, M.; Chakrabarti, R.; Hadjiev, V. G.; Palmer, J. C.; Vekilov, P. G. How to Identify the Crystal Growth Unit. *Israel J. Chem.* **2021**, *61* (11–12), 818–827.
- (200) Snyder, R. C.; Doherty, M. F. Faceted crystal shape evolution during dissolution or growth. *AIChE J.* **2007**, *53* (5), 1337–1348.
- (201) Sun, Y. Y.; Tilbury, C. J.; Reutzel-Edens, S. M.; Bhardwaj, R. M.; Li, J. J.; Doherty, M. F. Modeling Olanzapine Solution Growth Morphologies. *Cryst. Growth Des.* **2018**, *18* (2), 905–911.
- (202) Cuppen, H. M.; Meekes, H.; van Veenendaal, E.; van Enckevort, W. J. P.; Bennema, P.; Reedijk, M. F.; Arsic, J.; Vlieg, E. Kink density and propagation velocity of the [010] step on the Kossel (100) surface. *Surf. Sci.* **2002**, *506* (3), 183–195.
- (203) Padwal, N. A.; Doherty, M. F. Simple Accurate Non-equilibrium Step Velocity Model for Crystal Growth of Symmetric Organic Molecules. *Cryst. Growth Des.* **2022**, 22 (6), 3656–3661.
- (204) Zhang, J.; Nancollas, G. H. Kink Density and Rate of Step Movement during Growth and Dissolution of an ABCrystal in a Nonstoichiometric Solution. *J. Colloid Interface Sci.* **1998**, 200 (1), 131–145.
- (205) Kuvadia, Z. B.; Doherty, M. F. Spiral Growth Model for Faceted Crystals of Non-Centrosymmetric Organic Molecules Grown from Solution. *Cryst. Growth Des.* **2011**, *11* (7), 2780–2802.
- (206) Tilbury, C. J.; Joswiak, M. N.; Peters, B.; Doherty, M. F. Modeling Step Velocities and Edge Surface Structures during Growth of Non-Centrosymmetric Crystals. *Cryst. Growth Des.* **2017**, *17* (4), 2066–2080
- (207) Cuppen, H. M.; Meekes, H.; van Enckevort, W. J. P.; Vlieg, E. Kink incorporation and step propagation in a non-Kossel model. *Surf. Sci.* **2004**, *571* (1), 41–62.
- (208) Shim, H.-M.; Koo, K.-K. Crystal Morphology Prediction of Hexahydro-1,3,5-trinitro-1,3,5-triazine by the Spiral Growth Model. *Cryst. Growth Des.* **2014**, *14* (4), 1802–1810.
- (209) Shim, H.-M.; Kim, H.-S.; Koo, K.-K. Molecular Modeling on Supersaturation-Dependent Growth Habit of 1,1-Diamino-2,2-dinitroethylene. *Cryst. Growth Des.* **2015**, *15* (4), 1833–1842.
- (210) Shim, H.-M.; Koo, K.-K. Molecular Approach to the Effect of Interfacial Energy on Growth Habit of  $\varepsilon$ -HNIW. *Cryst. Growth Des.* **2016**, *16* (11), 6506–6513.
- (211) Zhao, Y. S.; Tilbury, C. J.; Landis, S.; Sun, Y. Y.; Li, J. J.; Zhu, P.; Doherty, M. F. A New Software Framework for Implementing Crystal Growth Models to Materials of Any Crystallographic Complexity. *Cryst. Growth Des.* **2020**, *20* (5), 2885–2892.
- (212) Hill, A. R.; Cubillas, P.; Gebbie-Rayet, J. T.; Trueman, M.; de Bruyn, N.; al Harthi, Z.; Pooley, R. J. S.; Attfield, M. P.; Blatov, V. A.; Proserpio, D. M.; Gale, J. D.; et al. CrystalGrower: A generic computer program for Monte Carlo modelling of crystal growth. *Chem. Sci.* **2021**, *12* (3), 1126–1146.
- (213) Stack, A. G.; Raiteri, P.; Gale, J. D. Accurate Rates of the Complex Mechanisms for Growth and Dissolution of Minerals Using a Combination of Rare-Event Theories. *J. Am. Chem. Soc.* **2012**, *134* (1), 11–14.

- (214) Joswiak, M. N.; Peters, B.; Doherty, M. F. In Silico Crystal Growth Rate Prediction for NaCl from Aqueous Solution. *Cryst. Growth Des.* **2018**, *18* (10), 6302–6306.
- (215) Kuvadia, Z. B.; Doherty, M. F. Reformulating multidimensional population balances for predicting crystal size and shape. *AIChE J.* **2013**, *59* (9), 3468–3474.
- (216) Marinova, V.; Wood, G. P. F.; Marziano, I.; Salvalaglio, M. Dynamics and Thermodynamics of Ibuprofen Conformational Isomerism at the Crystal/Solution Interface. *J. Chem. Theory Comput.* **2018**, *14* (12), 6484–6494.
- (217) Peters, B. Reaction Rate Theory and Rare Events Simulations; Elsevier, 2017.
- (218) Hall, S. W.; Díaz Leines, G.; Sarupria, S.; Rogal, J. Practical guide to replica exchange transition interface sampling and forward flux sampling. *J. Chem. Phys.* **2022**, *156* (20), 200901.
- (219) ten Wolde, P. R.; Frenkel, D. Computer simulation study of gas—liquid nucleation in a Lennard-Jones system. *J. Chem. Phys.* **1998**, 109 (22), 9901—9918.
- (220) ten Wolde, P. R.; Ruiz-Montero, M. J.; Frenkel, D. Numerical calculation of the rate of crystal nucleation in a Lennard-Jones system at moderate undercooling. *J. Chem. Phys.* **1996**, *104* (24), 9932–9947.
- (221) Auer, S.; Frenkel, D. Quantitative Prediction Of Crystal-Nucleation Rates For Spherical Colloids: A Computational Approach. *Annu. Rev. Phys. Chem.* **2004**, *55* (1), 333–361.
- (222) Salvalaglio, M.; Tiwary, P.; Maggioni, G. M.; Mazzotti, M.; Parrinello, M. Overcoming time scale and finite size limitations to compute nucleation rates from small scale well tempered metadynamics simulations. *J. Chem. Phys.* **2016**, *145* (21), 211925.
- (223) Agarwal, V.; Peters, B. Solute Precipitate Nucleation: A Review of Theory and Simulation Advances. *Adv. Chem. Phys.* **2014**, 97–160.
- (224) Fan, Z.; Men, H. An Overview on Atomistic Mechanisms of Heterogeneous Nucleation. *Metals* **2022**, *12*, 1547.
- (225) Salvalaglio, M.; Mazzotti, M.; Parrinello, M. Urea homogeneous nucleation mechanism is solvent dependent. *Faraday Discuss*. **2015**, *179*, 291–307.
- (226) Anwar, J.; Zahn, D. Uncovering Molecular Processes in Crystal Nucleation and Growth by Using Molecular Simulation. *Angew. Chem., Int. Ed.* **2011**, *50* (9), 1996–2013.
- (227) Davey, R. J.; Schroeder, S. L.; ter Horst, J. H. Nucleation of Organic CrystalsA Molecular Perspective. *Angew. Chem., Int. Ed.* **2013**, 52 (8), 2166–2179.
- (228) Cheng, B.; Tribello, G. A.; Ceriotti, M. Solid-liquid interfacial free energy out of equilibrium. *Phys. Rev. B* **2015**, 92 (18), 180102.
- (229) Karthika, S.; Radhakrishnan, T. K.; Kalaichelvi, P. A Review of Classical and Nonclassical Nucleation Theories. *Cryst. Growth Des.* **2016**, *16* (11), 6663–6681.
- (230) Nucleation in Condensed Matter: Applications in Materials and Biology, Kelton, K. F.; Greer, A. L., Eds.; Pergamon, 2010.
- (231) Kashchiev, D. Nucleation; Butterworth-Heinemann, 2000.
- (232) Zimmermann, N. E. R.; Vorselaars, B.; Espinosa, J. R.; Quigley, D.; Smith, W. R.; Sanz, E.; Vega, C.; Peters, B. NaCl nucleation from brine in seeded simulations: Sources of uncertainty in rate estimates. *J. Chem. Phys.* **2018**, *148* (22), 222838.
- (233) Knott, B. C.; Molinero, V.; Doherty, M. F.; Peters, B. Homogeneous Nucleation of Methane Hydrates: Unrealistic under Realistic Conditions. *J. Am. Chem. Soc.* **2012**, *134* (48), 19544–19547.
- (234) Duff, N.; Peters, B. Polymorph specific RMSD local order parameters for molecular crystals and nuclei: a-, b-, and c- glycine. *J. Chem. Phys.* **2011**, *135* (13), 134101.
- (235) Knott, B. C.; Duff, N.; Doherty, M. F.; Peters, B. Estimating diffusivity along a reaction coordinate in the high friction limit: Insights on pulse times in laser-induced nucleation. *J. Chem. Phys.* **2009**, *131* (22), 224112.
- (236) Nucleation Theory and Applications, Schmelzer, J. W. P., Eds.; WILEY-VCH Verlag GmbH & Co.KGaA, 2005.
- (237) Kalikmanov, V. I. Nucleation Theory; Springer, 2013.

- (238) Garside, J.; Davey, R. J. Invited Review Secondary Contact Nucleation: Kinetics, Growth And Scale-Up. *Chem. Eng. Commun.* **1980**, *4* (4–5), 393–424.
- (239) Hounslow, M. J. Nucleation, growth, and aggregation rates from steady-state experimental data. *AIChE J.* **1990**, *36* (11), 1748–1752.
- (240) Punnathanam, S.; Monson, P. A. Crystal nucleation in binary hard sphere mixtures: A Monte Carlo simulation study. *J. Chem. Phys.* **2006**, *125* (2), 024508.
- (241) Lifanov, Y.; Vorselaars, B.; Quigley, D. Nucleation barrier reconstruction via the seeding method in a lattice model with competing nucleation pathways. *J. Chem. Phys.* **2016**, *145* (21), 211912.
- (242) Sanz, E.; Vega, C.; Espinosa, J. R.; Caballero-Bernal, R.; Abascal, J. L. F.; Valeriani, C. Homogeneous Ice Nucleation at Moderate Supercooling from Molecular Simulation. *J. Am. Chem. Soc.* **2013**, *135* (40), 15008–15017.
- (243) Liu, C. X.; Wood, G. P. F.; Santiso, E. E. Modelling nucleation from solution with the string method in the osmotic ensemble. *Mol. Phys.* **2018**, *116* (21–22), 2998–3007.
- (244) ten Wolde, P. R.; Frenkel, D. Enhancement of Protein Crystal Nucleation by Critical Density Fluctuations. *Science* **1997**, 277 (5334), 1975–1978.
- (245) Vekilov, P. G. Two-step mechanism for the nucleation of crystals from solution. *J. Cryst. Growth* **2005**, 275 (1), 65–76.
- (246) Bosetti, L.; Mazzotti, M. Population Balance Modeling of Growth and Secondary Nucleation by Attrition and Ripening. *Cryst. Growth Des.* **2020**, 20 (1), 307–319.
- (247) Ahn, B.; Bosetti, L.; Mazzotti, M. Secondary Nucleation by Interparticle Energies. III. Nucleation Rate Model. *Cryst. Growth Des.* **2022**, 22 (6), 3625–3636.
- (248) Xu, S.; Hou, Z.; Chuai, X.; Wang, Y. Overview of Secondary Nucleation: From Fundamentals to Application. *Ind. Eng. Chem. Res.* **2020**, *59* (41), 18335–18356.
- (249) Industrial Crystallization, Mullin, J. W., Eds.; Springer, 1976.
- (250) Hoffmann, J.; Flannigan, J.; Cashmore, A.; Briuglia; Maria, L.; Steendam, R. R. E.; Gerard, C. J. J.; Haw, M. D.; Sefcik, J.; ter Horst, J. H. The unexpected dominance of secondary over primary nucleation. *Faraday Discuss.* **2022**, 235, 109–131.
- (251) Bal, V.; Peters, B. Crystallization with Sinusoidal Modulation of Stirrer Speed: Frequency Response Analysis and Secondary Nucleation Kinetics. *Cryst. Growth Des.* **2021**, *21* (1), 235–242.
- (252) Kiely, E.; Zwane, R.; Fox, R.; Reilly, A. M.; Guerin, S. Density functional theory predictions of the mechanical properties of crystalline materials. *CrystEngComm* **2021**, 23 (34), 5697–5710.
- (253) Crystallization Technology Handbook, Mersmann, A., Ed.; Marcel Dekker, Inc, 2001.
- (254) Turnbull, D. Phase Changes. In *Solid State Physics*, Seitz, F.; Turnbull, D., Ed.; Academic Press, 1956; Vol. 3, pp. 225306.
- (255) Cabriolu, R.; Li, T. Ice nucleation on carbon surface supports the classical theory for heterogeneous nucleation. *Phys. Rev. E* **2015**, 91 (5), 052402.
- (256) Auer, S.; Frenkel, D. Line Tension Controls Wall-Induced Crystal Nucleation in Hard-Sphere Colloids. *Phys. Rev. Lett.* **2003**, *91* (1), 015703.
- (257) Navascués, G.; Tarazona, P. Line tension effects in heterogeneous nucleation theory. *J. Chem. Phys.* **1981**, 75 (5), 2441–2446.
- (258) Mithen, J. P.; Sear, R. P. Computer simulation of epitaxial nucleation of a crystal on a crystalline surface. *J. Chem. Phys.* **2014**, 140 (8), 084504.
- (259) Turnbull, D.; Vonnegut, B. Nucleation Catalysis. *Ind. Eng. Chem.* **1952**, 44 (6), 1292–1298.
- (260) Fletcher, N. H. Size Effect in Heterogeneous Nucleation. J. Chem. Phys. 1958, 29 (3), 572–576.
- (261) Lupi, L.; Hudait, A.; Molinero, V. Heterogeneous Nucleation of Ice on Carbon Surfaces. *J. Am. Chem. Soc.* **2014**, *136* (8), 3156–3164.

(262) Fitzner, M.; Sosso, G. C.; Cox, S. J.; Michaelides, A. The Many Faces of Heterogeneous Ice Nucleation: Interplay Between Surface Morphology and Hydrophobicity. *J. Am. Chem. Soc.* **2015**, *137* (42), 13658–13669.

Article

- (263) Lupi, L.; Molinero, V. Does Hydrophilicity of Carbon Particles Improve Their Ice Nucleation Ability? *J. Phys. Chem. A* **2014**, 118 (35), 7330–7337.
- (264) Sosso, G. C.; Li, T.; Donadio, D.; Tribello, G. A.; Michaelides, A. Microscopic Mechanism and Kinetics of Ice Formation at Complex Interfaces: Zooming in on Kaolinite. *J. Phys. Chem. Lett.* **2016**, 7 (13), 2350–2355.
- (265) Lochhead, M. J.; Letellier, S. R.; Vogel, V. Assessing the Role of Interfacial Electrostatics in Oriented Mineral Nucleation at Charged Organic Monolayers. *J. Phys. Chem. B* **1997**, *101* (50), 10821–10827.
- (266) DeFever, R. S.; Sarupria, S. Surface chemistry effects on heterogeneous clathrate hydrate nucleation: A molecular dynamics study. *J. Chem. Thermodyn.* **2018**, *117*, 205–213.
- (267) Glatz, B.; Sarupria, S. Heterogeneous Ice Nucleation: Interplay of Surface Properties and Their Impact on Water Orientations. *Langmuir* **2018**, 34 (3), 1190–1198.
- (268) Cantor, B. Heterogeneous nucleation and adsorption. *Philos. T. R. Soc. A* **2003**, 361 (1804), 409–417.
- (269) Tang, S. K.; Davey, R. J.; Sacchi, P.; Cruz-Cabeza, A. J. Can molecular flexibility control crystallization? The case of para substituted benzoic acids. *Chem. Sci.* **2021**, *12* (3), 993–1000.
- (270) Mullin, J. W.; Nývlt, J. Programmed cooling of batch crystallizers. *Chem. Eng. Sci.* **1971**, 26 (3), 369–377.
- (271) Ward, J. D.; Yu, C.-C.; Doherty, M. F. A new framework and a simpler method for the development of batch crystallization recipes. *AIChE J.* **2011**, *57* (3), 606–617.
- (272) Ward, J. D.; Yu, C.-C.; Doherty, M. F. Erratum. AIChE J. **2012**, 58 (4), 1311–1311.
- (273) Deck, L.-T.; Hosseinalipour, M. S.; Mazzotti, M. Exact and Ubiquitous Condition for Solid-State Deracemization in Vitro and in Nature. *J. Am. Chem. Soc.* **2024**, *146* (6), 3872–3882.
- (274) Nagy, Z. K.; Braatz, R. D. Advances and New Directions in Crystallization Control. *Annu. Rev. Chem. Biomol.* **2012**, *3*, 55–75.
- (275) Farmer, T. C.; Carpenter, C. L.; Doherty, M. F. Polymorph selection by continuous crystallization. *AIChE J.* **2016**, *62* (9), 3505–3514.
- (276) Farmer, T. C.; Schiebel, S. K.; Chmelka, B. F.; Doherty, M. F. Polymorph Selection by Continuous Precipitation. *Cryst. Growth Des.* **2018**, *18* (8), 4306–4319.
- (277) Li, Y.; O'Shea, S.; Yin, Q.; Vetter, T. Polymorph Selection by Continuous Crystallization in the Presence of Wet Milling. *Cryst. Growth Des.* **2019**, *19* (4), 2259–2271.
- (278) Achermann, R.; Košir, A.; Bodák, B.; Bosetti, L.; Mazzotti, M. Process Performance and Operational Challenges in Continuous Crystallization: A Study of the Polymorphs of L-Glutamic Acid. *Cryst. Growth Des.* **2023**, 23 (4), 2485–2503.
- (279) Botsaris, G. D.; Mason, E. A.; Reid, R. C. Growth of Potassium Chloride Crystals from Aqueous Solutions. I. The Effect of Lead Chloride. *J. Chem. Phys.* **1966**, 45 (6), 1893–1899.
- (280) Dowling, R.; Davey, R. J.; Curtis, R. A.; Han, G. J.; Poornachary, S. K.; Chow, P. S.; Tan, R. B. H. Acceleration of crystal growth rates: an unexpected effect of tailor-made additives. *Chem. Commun.* **2010**, 46 (32), 5924–5926.
- (281) Li, L.; Lechuga-Ballesteros, D.; Szkudlarek, B. A.; Rodríguez-Hornedo, N. The Effect of Additives on Glycine Crystal Growth Kinetics. *J. Colloid Interface Sci.* **1994**, *168* (1), 8–14.
- (282) Piana, S.; Jones, F.; Gale, J. D. Aspartic acid as a crystal growth catalyst. *CrystEngComm* **2007**, *9* (12), 1187–1191.
- (283) Michaels, A. S.; Colville, A. R., Jr. The Effect Of Surface Active Agents On Crystal Growth Rate And Crystal Habit. *J. Phys. Chem.* **1960**, *64* (1), 13–19.
- (284) Davey, R. J.; Black, S. N.; Logan, D.; Maginn, S. J.; Fairbrother, J. E.; Grant, D. J. W. Structural and kinetic features of

- crystal growth inhibition: Adipic acid growing in the presence of nalkanoic acids. *J. Chem. Soc. Faraday T* **1992**, 88 (23), 3461–3466.
- (285) Shekunov, B. Y.; Grant, D. J. W.; Latham, R. J.; Sherwood, J. N. In Situ Optical Interferometric Studies of the Growth and Dissolution Behavior of Paracetamol (Acetaminophen) Crystals. 3. Influence of Growth in the Presence of p -Acetoxyacetanilide. *J. Phys. Chem. B* 1997, 101 (44), 9107–9112.
- (286) Ma, W.; Lutsko, J. F.; Rimer, J. D.; Vekilov, P. G. Antagonistic cooperativity between crystal growth modifiers. *Nature* **2020**, *577* (7791), 497–501.
- (287) Kuvadia, Z. B.; Doherty, M. F. Effect of Structurally Similar Additives on Crystal Habit of Organic Molecular Crystals at Low Supersaturation. *Cryst. Growth Des.* **2013**, *13* (4), 1412–1428.
- (288) Lutsko, J. F.; González-Segredo, N.; Durán-Olivencia, M. A.; Maes, D.; Van Driessche, A. E. S.; Sleutel, M. Crystal Growth Cessation Revisited: The Physical Basis of Step Pinning. *Cryst. Growth Des.* **2014**, *14* (11), 6129–6134.
- (289) Shtukenberg, A. G.; Ward, M. D.; Kahr, B. Crystal growth inhibition by impurity stoppers, now. *J. Cryst. Growth* **2022**, 597, 126839.
- (290) Mazal, T.; Doherty, M. F. Modeling Impurity-Mediated Crystal Growth and Morphologies of Centrosymmetric Molecules. *Cryst. Growth Des.* **2023**, 23 (1), 369–379.
- (291) Agrawal, P.; Rawal, S. H.; Reddy, V. R.; Viswanath, S. K.; Merritt, J. M. Case Studies in the Application of a Workflow-Based Crystallization Design for Optimized Impurity Rejection in Pharmaceutical Development. *Org. Process Res. Dev.* **2023**, 27 (4), 610–626.
- (292) Nordstrom, F. L.; Sirota, E.; Hartmanshenn, C.; Kwok, T. T.; Paolello, M.; Li, H.; Abeyta, V.; Bramante, T.; Madrigal, E.; Behre, T.; et al. Prevalence of Impurity Retention Mechanisms in Pharmaceutical Crystallizations. *Org. Process Res. Dev.* **2023**, *27* (4), 723–741.
- (293) Urwin, S. J.; Levilain, G.; Marziano, I.; Merritt, J. M.; Houson, I.; ter Horst, J. H. A Structured Approach To Cope with Impurities during Industrial Crystallization Development. *Org. Process Res. Dev.* **2020**, 24 (8), 1443–1456.
- (294) Shiea, M.; Buffo, A.; Vanni, M.; Marchisio, D. Numerical Methods for the Solution of Population Balance Equations Coupled with Computational Fluid Dynamics. *Annu. Rev. Chem. Biomol.* **2020**, *11* (1), 339–366.
- (295) Fox, R. O. Computational Models for Turbulent Reacting Flows; Cambridge University Press, 2003.
- (296) Fox, R. O. Large-Eddy-Simulation Tools for Multiphase Flows. *Annu. Rev. Fluid. Mech.* **2012**, 44 (1), 47–76.
- (297) Achermann, R.; Adams, R.; Prasser, H.-M.; Mazzotti, M. Characterization of a small-scale crystallizer using CFD simulations and X-ray CT measurements. *Chem. Eng. Sci.* **2022**, 256, 117697.
- (298) Zhang, M.; Liang, Z. Z.; Wu, F.; Chen, J. F.; Xue, C. Y.; Zhao, H. Crystal engineering of ibuprofen compounds: From molecule to crystal structure to morphology prediction by computational simulation and experimental study. *J. Cryst. Growth* **2017**, *467*, 47–53.
- (299) van der Lee, A.; Dumitrescu, D. G. Thermal expansion properties of organic crystals: a CSD study. *Chem. Sci.* **2021**, *12* (24), 8537–8547.
- (300) Kriz, K.; Schmidt, L.; Andersson, A. T.; Walz, M.-M.; van der Spoel, D. An Imbalance in the Force: The Need for Standardized Benchmarks for Molecular Simulation. *J. Chem. Inf. Model.* **2023**, 63 (2), 412–431.
- (301) James, A.; John, C.; Melekamburath, A.; Rajeevan, M.; Swathi, R. S. A journey toward the heaven of chemical fidelity of intermolecular force fields. *Wiley Interdiscip. Rev.: Comput. Mol. Sci.* **2022**, *12* (4), No. e1599.
- (302) Aina, A. A.; Misquitta, A. J.; Price, S. L. A non-empirical intermolecular force-field for trinitrobenzene and its application in crystal structure prediction. *J. Chem. Phys.* **2021**, *154* (9), 094123.
- (303) Uzoh, O. G.; Galek, P. T. A.; Price, S. L. Analysis of the conformational profiles of fenamates shows route towards novel, higher accuracy, force-fields for pharmaceuticals. *Phys. Chem. Chem. Phys.* **2015**, *17* (12), 7936–7948.

- (304) Maurer, R. J.; Freysoldt, C.; Reilly, A. M.; Brandenburg, J. G.; Hofmann, O. T.; Bjorkman, T.; Lebegue, S.; Tkatchenko, A.; Clarke, D. R. Advances in Density-Functional Calculations for Materials Modeling. *Annu. Rev. Mater. Res.* **2019**, *49*, 1–30.
- (305) Hoja, J.; Ko, H.-Y.; Neumann, M. A.; Car, R.; DiStasio, R. A.; Tkatchenko, A. Reliable and practical computational description of molecular crystal polymorphs. *Sci. Adv.* **2019**, *5* (1), No. eaau—3338. (306) Beran, G. J. O. Modeling Polymorphic Molecular Crystals with Electronic Structure Theory. *Chem. Rev.* **2016**, *116* (9), 5567—
- (307) Hunnisett, L. M., et al.. The Seventh Blind Test of Crystal Structure Prediction: Structure Generation Methods, *Acta Crystallogr. B*, **2024**.
- (308) Hunnisett, L. M. et al.. The Seventh Blind Test of Crystal Structure Prediction: Structure Ranking Methods. *Acta Crystallogr. B.* **2024**.
- (309) Price, L. S.; Price, S. L. Packing Preferences of Chalcones: A Model Conjugated Pharmaceutical Scaffold. *Cryst. Growth Des.* **2022**, 22 (3), 1801–1816.
- (310) Bhardwaj, R. M.; McMahon, J. A.; Nyman, J.; Price, L. S.; Konar, S.; Oswald, I. D. H.; Pulham, C. R.; Price, S. L.; Reutzel-Edens, S. M. A Prolific Solvate Former, Galunisertib, under the Pressure of Crystal Structure Prediction, Produces Ten Diverse Polymorphs. J. Am. Chem. Soc. 2019, 141 (35), 13887–13897.
- (311) Braun, D. E.; Oberarcher, H.; Arnhard, K.; Orlova, M.; Griesser, U. J. 4-Aminoquinaldine monohydrate polymorphism: Prediction and impurity aided discovery of a difficult to access stable form. *CrystEngComm* **2016**, *18*, 4053–4067.
- (312) Braun, D. E.; Vickers, M.; Griesser, U. J. Dapsone Form V: A Late Appearing Thermodynamic Polymorph of a Pharmaceutical. *Mol. Pharmaceut* **2019**, *16* (7), 3221–3236.
- (313) Burcham, C. L. Crystalline compound and a process for its preparation US 8,299,059 B2 2012.